

ABSTRACT

DIGITAL IMAGE PROCESSING: HOMOMORPHIC IMAGE ENHANCEMENT, IMAGE RESTORATION AND PHASE-ONLY IMAGE PROCESSING

by James Jianzhou Long

Homomorphic image processing is of interest in contrast enhancement and controlling dynamic range. A simple scatter model was established and a homomorphic filter was discussed in the different cases of contrast enhancement and dynamic range compression.

Image restoration is to design a restored filter for the inverse problem. A general degradation model was discussed and three types of filters were derived: the inverse filter, the Wiener filter, and the magnitude-only filter. A derivation for the Wiener filter in the spatial domain was developed. The advantages and disadvantages of these filters were compared. These filters were applied to degraded pictures to obtain image restoration. The relationship between the frequency resolution and statistical resolution of the ensemble averaging magnitude-only filter with the different windows size and overlap were demonstrated.

Phase-only image processing was contrasted with magnitude-only image processing to emphasize the importance of phase information in image synthesis, restoration, and reconstruction. Examples of exact image reconstruction from phase-only spectra were shown. A comparison of phase-only, magnitude-only and classical matched filters under the different signal to noise ratio (SNR) situations were presented and image identification examples were provided.

**DIGITAL IMAGE PROCESSING:
HOMOMORPHIC IMAGE ENHANCEMENT, IMAGE
RESTORATION AND PHASE-ONLY IMAGE PROCESSING**

by

James Jianzhou Long

A Thesis Submitted
in Partial Fulfillment of the Requirements
for the degree of

Master of Science

Physics

Instrumentation

at

University of Wisconsin Oshkosh

Oshkosh, WI 54901

August 1994

DEAN OF THE GRADUATE SCHOOL

DATE COMMITTEE APPROVAL

Dee Hardhanson

8-5-94 Date Approved

7-28-94 John H. Karl Advisor

7/28/94 Roy R. Kuiper Member

7-28-94 Malinda Parnow Member

Date Format Approval

7-27-94 John I. Stapp

7A
1632
.164
C. 2.

**To my dear grandmother, parents,
brothers and sisters**

To my dear Y.C.C.

ACKNOWLEDGEMENTS

I would like to gratefully thank Dr. John Karl for supervising this thesis. Without the knowledge gained from his two digital signal processing classes, without the heuristic discussion with him, without his sharp perspective and expertise, without his enthusiastic support and encouragement, this paper would never have been completed.

I would like to express my very special thanks to Dr. Roy Knispel for his serving as my graduate advisor, giving his kindness, patience and encouragement through my whole graduate study and daily life. Without his remarkable contribution, his shining knowledge, his broad engagement, I would have never so successfully finished my study.

Thanks also to Dr. Merlin Passow and Dr. Sandra Gade and all other faculty for their consistent support and encouragement.

Finally, I would like to gratefully acknowledge my friends and classmates around me for their encouragement and assistance. Special thanks to Philip Salzman for his friendship and the wonderful time we spent.

Additionally I give special thanks to the kind readers who tolerate my English which suffers from my limited experience with this language.

TABLE OF CONTENTS

	Page
LIST OF TABLES v
LIST OF FIGURES vi
INTRODUCTION TO DIGITAL IMAGE PROCESSING 1
Spatial domain examples 3
Frequency domain examples 14
Mask design 17
HOMOMORPHIC IMAGE ENHANCEMENT 21
Introduction 21
Experiment 26
Conclusion 29
IMAGE RESTORATION 30
Introduction to image restoration 30
Inverse filter 36
Wiener filter 43
Magnitude-only inverse filter 53
Summary 61
PHASE-ONLY IMAGE PROCESSING 68
The important of phase in image synthesis 68
Image restoration via a true phase spectrum 79
Image reconstruction from phase-only information 85
Phase-only match filter and its applications 92
CONCLUSION 104
REFERENCES 106
APPENDIX 108

LIST OF TABLES

	Page
Table 3-1. Summary of the three types of restoration filters62
Table 4-1. The discrimination test of three matched filters100

LIST OF FIGURES

	Page
Figure 1-1: Equally weighted average smoothing5
Figure 1-2: Unsharp masking enhancement6
Figure 1-3: Shift and difference edge enhancement8
Figure 1-4: Gradient direction edge enhancement10
Figure 1-5: Laplacian edge enhancement11
Figure 1-6: Embossing enhancement13
Figure 1-7: Contour filtering enhancement15
Figure 1-8: Image filtering in the frequency domain18
Figure 2-1: Image scatter model22
Figure 2-2: Diagram of homomorphic image processing22
Figure 2-3: Homomorphic image processing: contrast enhancement and dynamic control27
Figure 3-1: The power spectrum of a noise image39
Figure 3-2: Examples of the inverse filter39
Figure 3-3: Examples of the Wiener filter51
Figure 3-4: Examples of magnitude-only inverse filter and ensemble averaging magnitude-only filter with SNR = 100058
Figure 3-5: Examples of magnitude-only inverse filter and ensemble averaging magnitude-only filter with SNR = 10059

	Page
Figure 3-6: Examples of ensemble averaging magnitude-only inverse filter with different window size and overlap length	.60
Figure 3-7: The example of the iterative Wiener filter66
Figure 4-1: Single picture's synthesis71
Figure 4-2: Pictures' cross synthesis72
Figure 4-3: Single high-geometry picture's synthesis74
Figure 4-4: High-geometry picture's synthesis75
Figure 4-5: Logarithm magnitude spectra of continuous grey tone pictures77
Figure 4-6: Logarithm magnitude spectra of high-geometry pictures	.78
Figure 4-7: Image restoration via power spectrum estimation .	.83
Figure 4-8: The iterative image reconstruction via the Fourier transform of the phase spectrum91
Figure 4-9: Autocorrelation's peak of three matched filters . .	.97
Figure 4-10: Pictures for the discrimination ability test101
Figure 4-11: Image restoration via matched filters103

CHAPTER I

INTRODUCTION TO DIGITAL IMAGE PROCESSING

What is image processing? Actually image processing is surrounding us every day. For example, the glasses we wear provide optical image processing which helps to correct our visual image; our TV's contrast or brightness adjustment provides electronic image processing which helps to make the pictures appealing to our eyes. Digital image processing is a similar kind of image processing in digital form, which uses numeric techniques to process images. Digital computers and digital signal processing (DSP) techniques have brought digital image processing into reality. All of the methods used by photographers, such as enhancement, manipulation and subtraction, can be done in the today's digital "darkroom".

The digital image processing problem is to find out proper digital operators, then carry out the operations. Seeking operators is simply thinking of a 2-dimensional digital filter design. Generally, there are three operations of interest in digital image processing: quality enhancement, analysis, and coding. Quality enhancement may be divided into two classes: one is to make the digital picture more appealing to our eyes, for example, making the images smooth or sharp. This is called image enhancement. The other is to recover

an image from a degraded version of the original one. For example, if a recorded picture is blurred due to the motion of the camera, then a digital operator is used to restore the degraded picture to the correct picture. This is called image restoration. Image analysis is an operation to describe an image and suggest a further operation. For example, a picture's information can be retrieved from its histogram, which is a function of the number of pixels or probability vs. pixels' intensity or brightness. A low contrast picture's histogram may only occupy a small region, then a technique called histogram equalization that tries to expand the histogram equally over the whole space, may be applied to the contrast enhancement (Gonzalez et al., 1987). Image coding is used because some images are too large to store and too long to transmit. For example, a 640x480 resolution picture of 256 grey scale requires 300 KB space. It may be necessary to change the image into another digital form in order to reduce its storage.

Since an operator is a digital filter, the corresponding image operations can be regarded as 2-D filtering. Linear shift invariant (LSI) filtering of our interest can be carried out by the convolution operation in either spatial domain or multiplication in frequency domain by discrete Fourier transform (DFT). The choice of operation depends on the trade off between the computing time and storage space.

Since digital image processing deals with the pictorial information, pictorial

demonstrations will provide deeper insight into image processing. We begin our discussion with some simple examples of image processing, using 3×3 operations. There are two very common image operations: smoothing and sharpening. Let us begin with these operations in the spatial domain, then in the frequency domain. All the sample pictures in this thesis are 256×256 pixels and with 256 grey scale for each pixel. The programs were written using the IDL programming language (Research System Inc., 1993) under the OpenWin environment on a Sun Sparc station.

Spatial domain examples

As we know, the integration helps to smooth the data. And the integration may be written as the addition of finite terms. Probably the simplest smoothing example is to replace each pixel with the equally weighted average of all its neighbors. Each smoothing operator may be represented as a 2-D matrix or mask $h(x,y)$. One of these masks is:

$$\begin{array}{ccccc} 1/9 & 1/9 & 1/9 & & h_{x-1,y-1} & h_{x-1,y} & h_{x-1,y+1} \\ 1/9 & 1/9 & 1/9 & \text{or} & h_{x,y-1} & h_{x,y} & h_{x,y+1} \\ 1/9 & 1/9 & 1/9 & & h_{x+1,y-1} & h_{x+1,y} & h_{x+1,y+1} \end{array}$$

The convolution between the operator $h(x,y)$ and the picture $f(x,y)$ carried in time domain will be

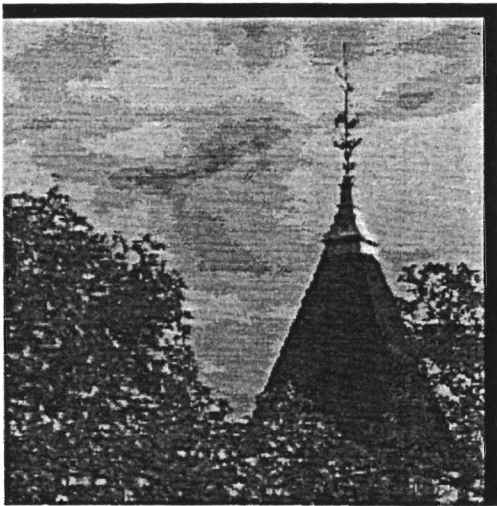
$$\begin{aligned}
 f(x,y) &= f(x,y) ** h(x,y) \\
 &= f_{x-1,y-1} * h_{x-1,y-1} + f_{x-1,y} * h_{x-1,y} + f_{x-1,y+1} * h_{x-1,y+1} \\
 &\quad + f_{x,y-1} * h_{x,y-1} + f_{x,y} * h_{x,y} + f_{x,y+1} * h_{x,y+1} \\
 &\quad + f_{x+1,y-1} * h_{x+1,y-1} + f_{x+1,y} * h_{x+1,y} + f_{x+1,y+1} * h_{x+1,y+1}
 \end{aligned}$$

where $**$ is the convolution operation and $f(x,y)$ is the processed picture. The result of this operation is shown in Figure 1-1. The processed picture is smoother or blurrier than its original one as expected. This process can be used to smooth spot noise (small areas of very bright pixels) in a picture (Long et al., 1992).

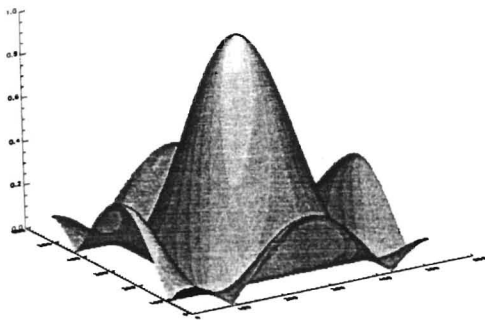
Sharpening, accentuation of the high frequency edge information in a picture, is the opposite operation of smoothing. Let us look at some very common sharpening masks. An unsharp masking enhancement mask is derived from the subtraction of a smooth picture from its original one. After subtraction the low frequency information, of course, the high frequency information remains in the original picture. A detailed derivation may be found in the mask design section. This mask is:

$$\begin{array}{ccc}
 0 & -1 & 0 \\
 -1 & 5 & -1 \\
 0 & -1 & 0
 \end{array}$$

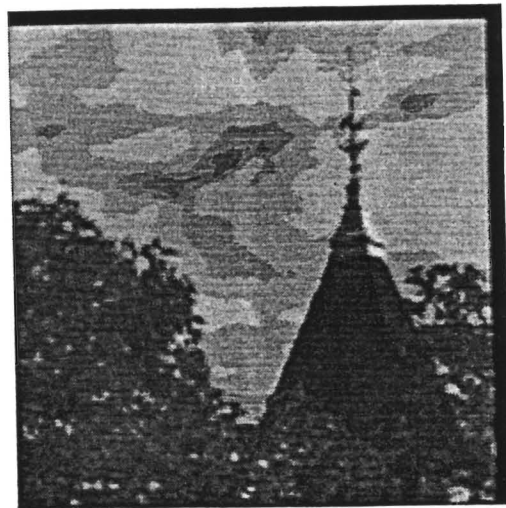
The result of this operation is shown in Figure 1-2. The edge information of the processed picture has been enhanced as expected. Some other sharpening



(a) The original picture 'UWO'

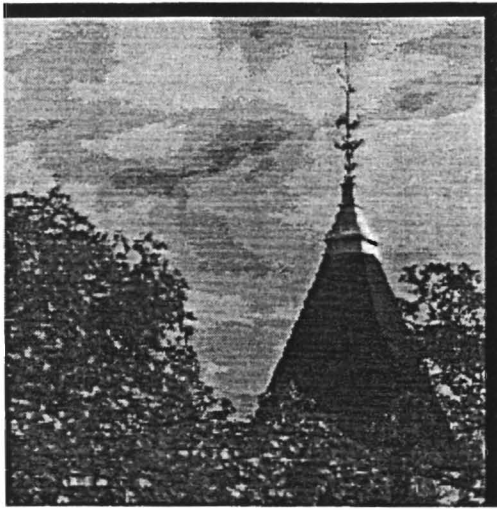


(b) The magnitude frequency response of the mask (ranging from $-\pi$ to π and zero frequency in the center of the plane)

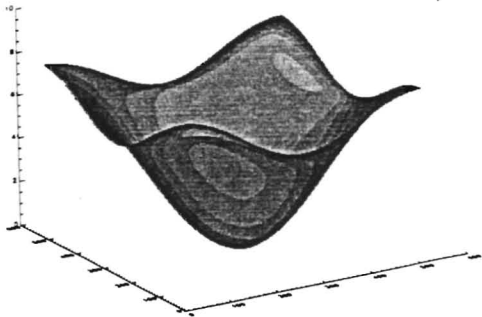


(c) The picture processed by the convolution with the mask

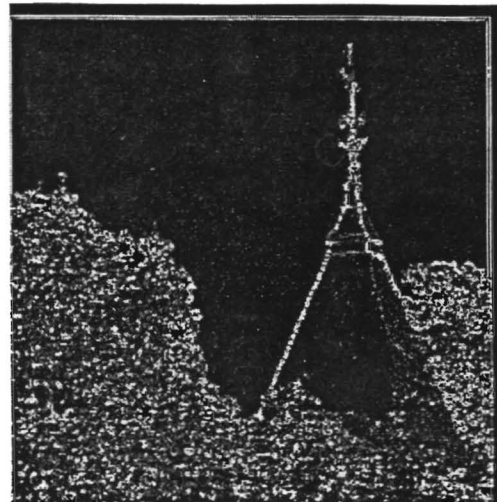
Fig. 1-1. Equally weighted average smoothing



(a) The original picture 'UWO'



(b) The magnitude frequency response of the mask (ranging from $-\pi$ to π and zero frequency in the center of the plane)



(c) The picture processed by the convolution with the mask

Fig. 1-2. Unsharp masking enhancement

operators of our interest are for the enhancement of edges in a certain direction, such as vertical, horizontal, gradient or all directions.

Shift and difference edge enhancement mask (Baxes, 1984), as the name implies, is to subtract a spatially shifted picture from its original one. For example, after subtraction of a vertically shifted picture from its original picture, the vertical edges will be enhanced. A vertical direction enhancement mask is listed below

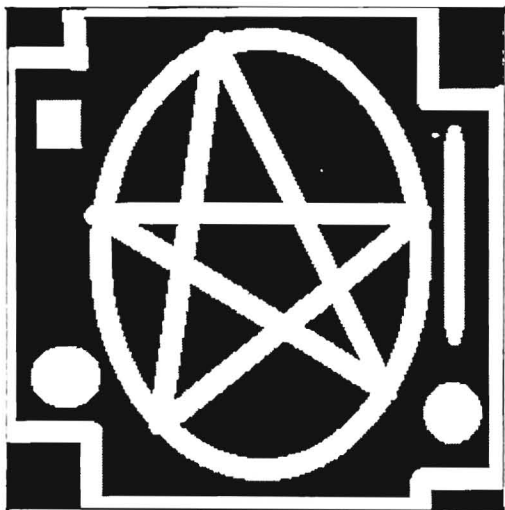
$$\begin{array}{ccc} 0 & -1 & 0 \\ 0 & 1 & 0 \\ 0 & 0 & 0 \end{array}$$

The example of using this mask is shown in Figure 1-3. The processed picture shows the edge enhancement in the vertical direction.

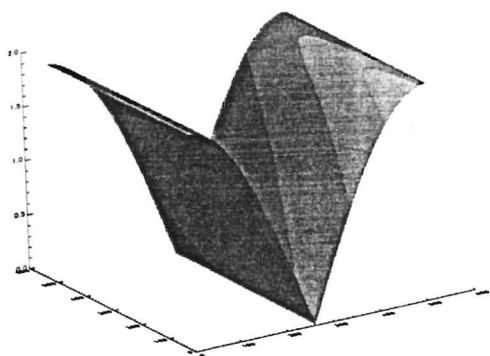
Gradient direction edge enhancement mask is similar to that of shift and different edge enhancement. For example, an east direction enhancement mask is

$$\begin{array}{ccc} -1 & 1 & 1 \\ -1 & -2 & 1 \\ -1 & 1 & 1 \end{array}$$

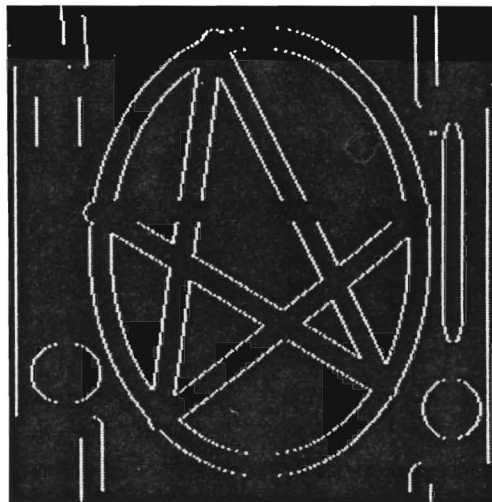
This mask can be rotated a certain degree to form another enhancement operator in another direction or gradient. For example, a 45-degree counterclockwise rotation of this east mask forms a northeast direction



(a) The original picture 'PATTEN'



(b) The magnitude frequency response of the mask (ranging from $-\pi$ to π and zero frequency in the center of the plane)



(c) The picture processed by the convolution with the mask

Fig. 1-3. Shift and difference edge enhancement

enhancement mask, which is

$$\begin{array}{ccc} 1 & 1 & 1 \\ -1 & -2 & 1 \\ -1 & -1 & 1 \end{array}$$

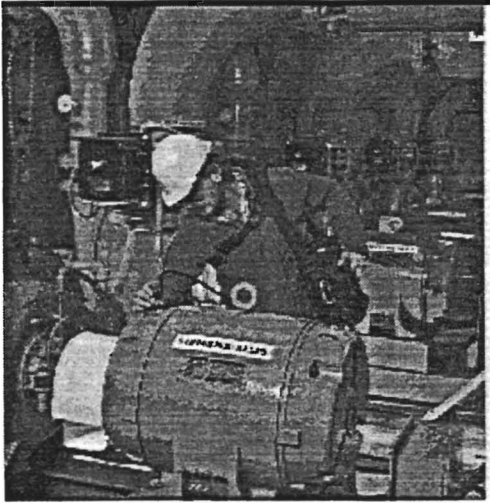
The result of this operation is shown in Figure 1-4. Unfortunately, the processed picture enhances the edge information not only in the northeast direction, but also in the northwest direction.

Laplacian mask is an omnidirectional enhancement operator. This highpass mask looks like:

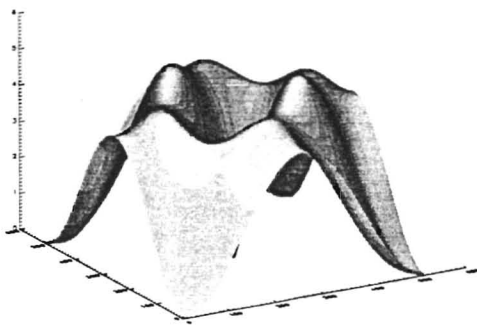
$$\begin{array}{ccc} 0 & -1 & 0 \\ -1 & 4 & -1 \\ 0 & -1 & 0 \end{array}$$

The lowpass Laplacian mask will be discussed in the mask design section and the highpass mask is simply formed from taking the minus sign of that of the lowpass mask. The expected result of this operation is shown in Figure 1-5.

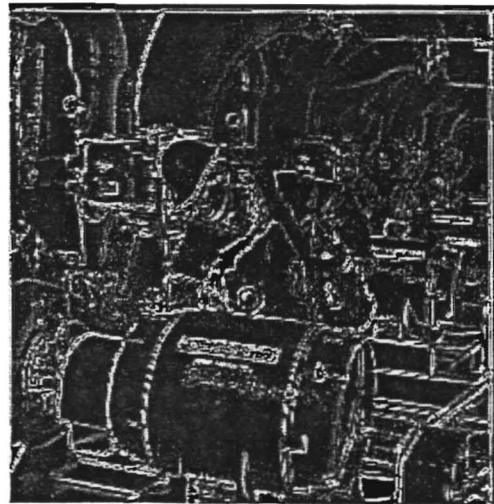
Embossing mask is to embolden a picture. The embossing picture should contain both the original information and the emphasis edge information. Thus this mask should reflect these characteristic. This mask is:



(a) The original picture 'MAN'



(b) The magnitude frequency response of the mask (ranging from $-\pi$ to π and zero frequency in the center of the plane)

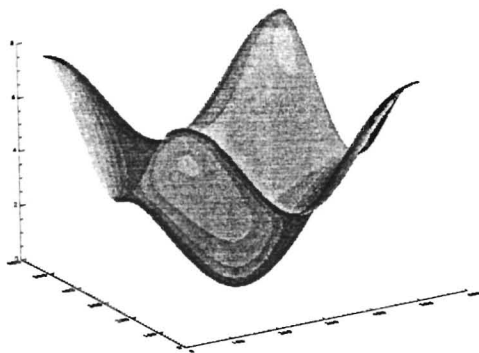


(c) The picture processed by the convolution with the mask

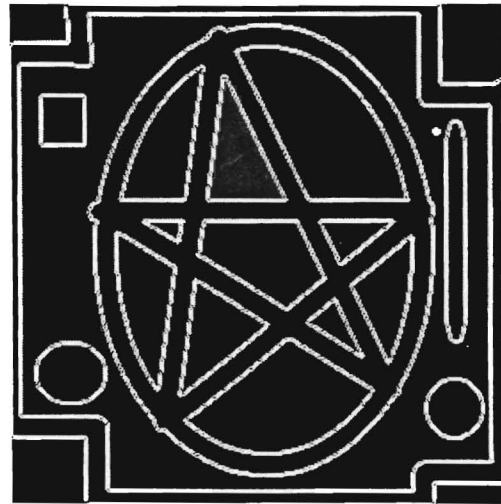
Fig. 1-4. Gradient direction edge enhancement



(a) The original picture 'PATTEN'



(b) The magnitude frequency response of the mask (ranging from $-\pi$ to π and zero frequency in the center of the plane)



(c) The picture processed by the convolution with the mask

Fig. 1-5. Laplacian edge enhancement

1	1	1
0	1	0
-1	-1	-1

The result of this example is illustrated in Figure 1-6. Obviously, all the edge information has been highlighted and it is mostly used in art design applications.

The last interesting edge enhancement operator is the contour filter (Watkins, 1993). This filter outlines all edges in a picture, that especially gives an impression of a contour mapping from an aeroplane picture. Thus, we call it contour filter. It is a non-linear filter. The new picture is calculated from

$$f(x,y) = \text{sqrt}\{ [f(x,y) ** h_v(x,y)]^2 + [f(x,y) ** h_h(x,y)]^2 \}$$

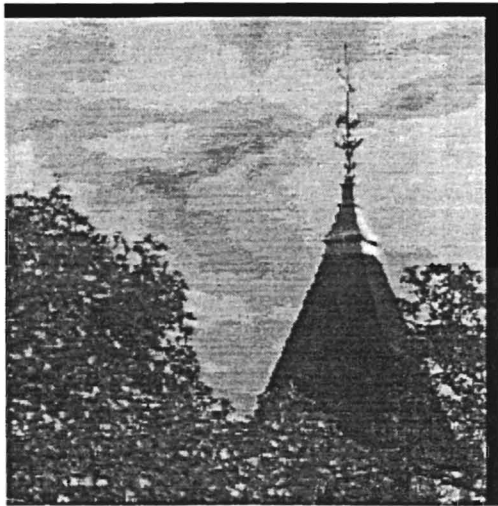
where h_h is a Sobel filter in the horizontal direction, which is

1	2	1
0	0	0
-1	-2	-1

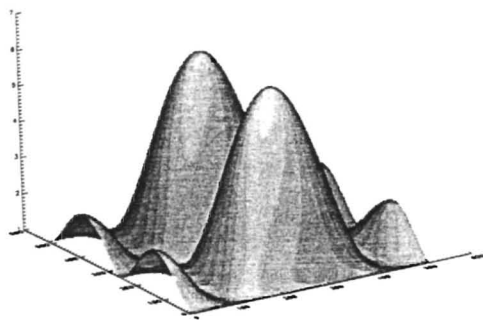
and h_v is a Sobel filter in vertical direction, which is

1	0	-1
2	0	-2
1	0	-1

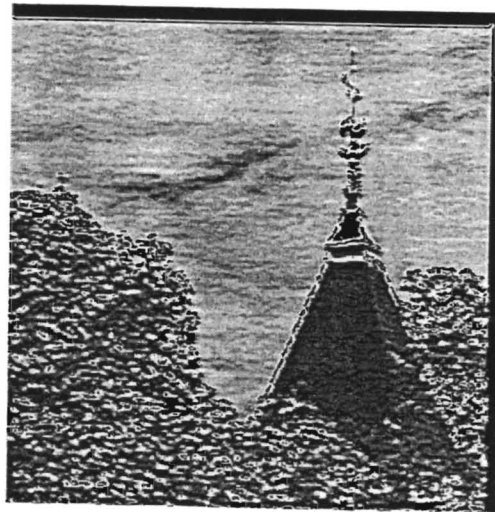
The contour filter is of great interest in some applications, such as remote sensing and geography information systems (GIS). The filtered picture is



(a) The original picture 'UWO'



(b) The magnitude frequency response of the mask (ranging from $-\pi$ to π and zero frequency in the center of the plane)



(c) The picture processed by the convolution with the mask

Fig. 1-6. Embossing enhancement

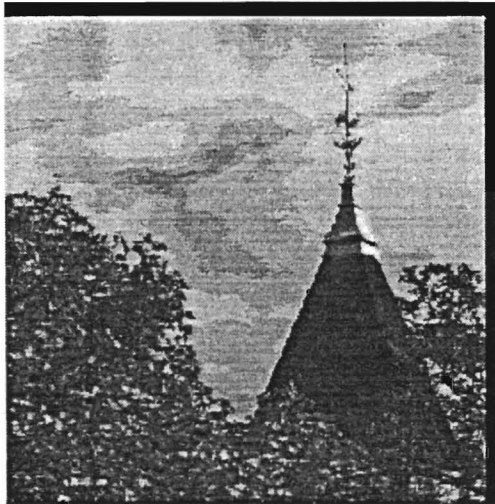
shown in Figure 1-7. The processed picture looks like a contour map, especially in the area of leaves. The edge enhancement technique can be applied in edge detection, which is very important in machine vision or image segmenting; it divides the image into many useful segments for further processing.

The above examples all use convolution in the spatial domain. But for LSI operations this filtering can also be accomplished in the frequency domain, which has frequently certain advantages.

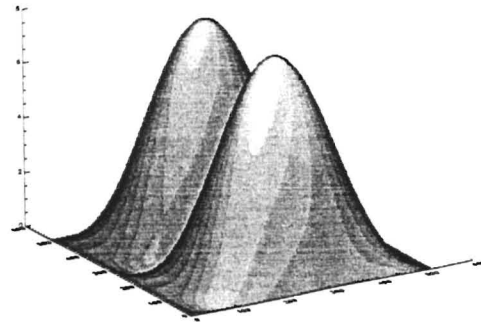
Frequency domain examples

Spatial domain image processing has the advantage of small storage space and fast computation time for short operators (regardless of the overhead of the frequent read and write operations on the storage devices). For example, the program of handling the 3x3 masks above only requires two 3x3 matrices to store both the operator and pixels. But when the operators are very large, computing time becomes a serious problem in the spatial domain.

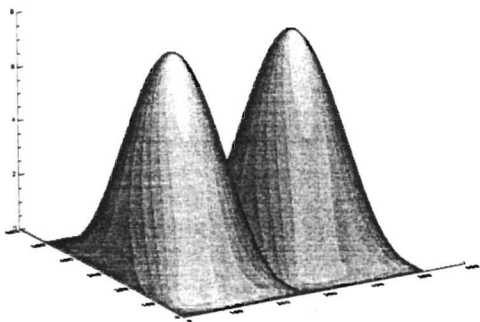
Additionally, short spatial domain operations are insufficient in complicated applications. This is why Fourier processing is so popular, and many image processing algorithms are carried out in the frequency domain. Also, frequency domain operations give a deeper insight of image processing. It is easy to understand what the above operators do while looking at the masks,



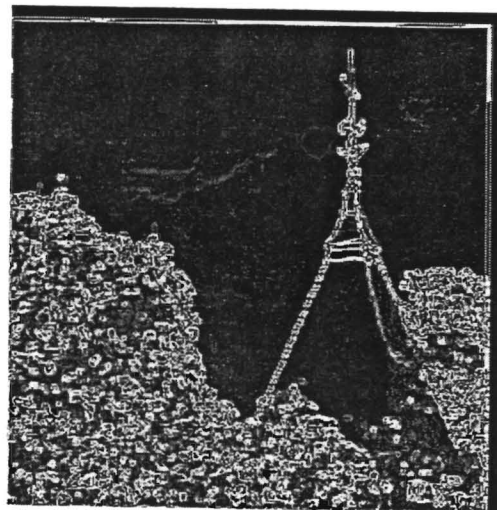
(a) The original picture 'UWO'



(b) The magnitude frequency response of the Sobel vertical filter (ranging from $-\pi$ to π and zero frequency in the center of the plane)



(c) The magnitude frequency response of the Sobel horizontal filter (ranging from $-\pi$ to π and zero frequency in the center of the plane)



(d) The picture processed by the Sobel filter

Fig. 1-7. Contour filtering enhancement

but if the masks are larger and more complex, it is difficult to tell their properties, such as the gain and cutoff frequency. Another problem arises, that is the above 3x3 masks are too small to control the frequency response precisely. The cutoff frequency is either too high or too low in the particular application, causing under- or over-filtering. A solution is found by specifying more points in the frequency domain, resulting in an equivalent larger mask in the spatial domain. A very common filter in the frequency domain is the Butterworth filter. The power spectrum response of its low-pass filter is presented as

$$|H(u, v)|^2 = \frac{1.0}{1.0 + \left[\frac{D(u, v)}{D_0} \right]^{2n}}$$

and its highpass filter's power spectrum response will be

$$|H(u, v)|^2 = \frac{1.0}{1.0 + \left[\frac{D_0}{D(u, v)} \right]^{2n}}$$

where D_0 is the cutoff frequency, and $D(u, v)$ is the discrete point along u and v directions in the frequency domain (that is $D^2(u, v) = u^2 + v^2$) and n is the order of the filter. The higher the order, the sharper transition band.

The resulting pictures and the filter's power spectrum response are shown in

Figure 1-8. We can see the filter has been very precisely defined according to the cutoff frequency and the filter's order.

Mask design

The longer spatial domain mask does a better job. In some applications, such as a build-in digital operator for noise filtering, the spatial domain masks become necessary since the masks are easy and time-efficient implemented. How can we derive the spatial domain mask? It is a problem of 2-D digital filter design. There are many publications covering this topic. Two of the general methods to derive the spatial domain masks are: from the differential equation, and from frequency sampling.

If the integration can be regarded as a smoothing operation, the derivative operation can be thought of as sharpening operation.

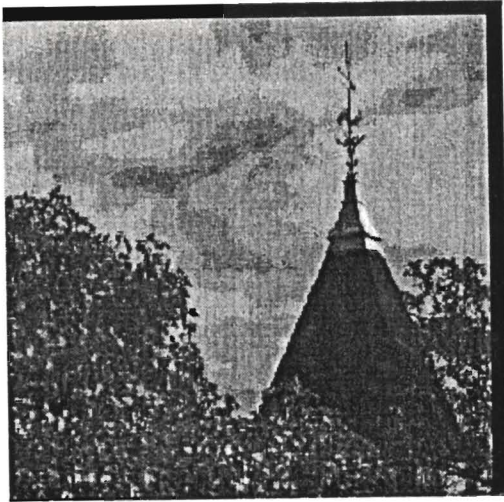
Let us begin with a 2-D Laplacian operation over a picture $f(x,y)$:

$$\nabla^2 f(x, y) = \frac{\partial^2 f(x, y)}{\partial x^2} + \frac{\partial^2 f(x, y)}{\partial y^2}$$

Defining the difference operators using forward differences gives

$$\frac{\partial f(x, y)}{\partial x} \rightarrow f(x+1, y) - f(x, y)$$

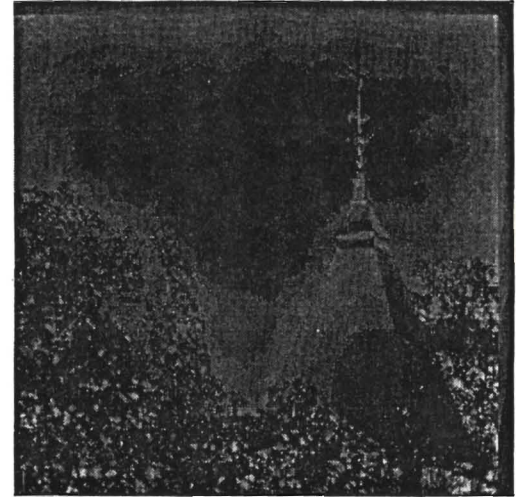
and



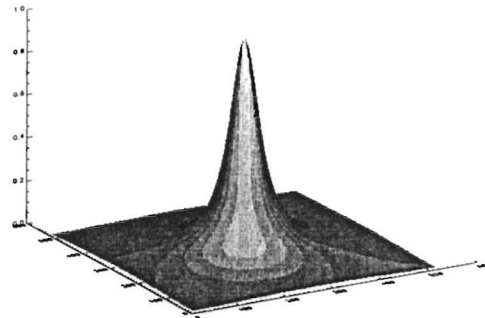
(a) The original picture 'UWO'



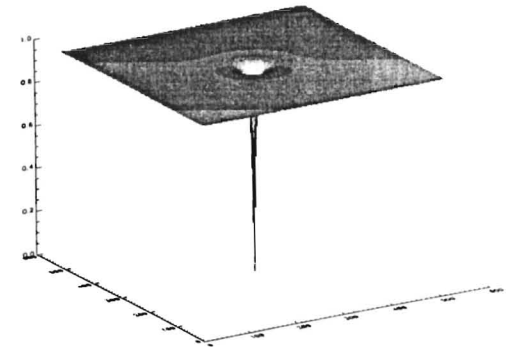
(c) The picture processed by the Butterworth lowpass filter



(e) The picture processed by the Butterworth highpass filter



(b) The magnitude frequency response of the Butterworth lowpass filter (ranging from $-\pi$ to π and zero frequency in the center of the plane)



(d) The magnitude frequency response of the Butterworth highpass filter (ranging from $-\pi$ to π and zero frequency in the center of the plane)

Fig. 1-8. Image filtering in the frequency domain

$$\frac{\partial f(x, y)}{\partial y} \rightarrow f(x, y+1) - f(x, y)$$

Then applying these approximations twice gives

$$\nabla^2 f(x, y) = f(x+1, y) + f(x-1, y) + f(x, y+1) + f(x, y-1) - 4f(x, y)$$

The result of the above processing is a blurred picture, which is the same as the convolution between a picture $f(x, y)$ and a mask $h(x, y)$. The mask is:

$$\begin{array}{ccc} 0 & 1 & 0 \\ 1 & -4 & 1 \\ 0 & 1 & 0 \end{array}$$

This mask is the same (except for an overall minus sign) as the Laplacian mask presented previously as an omnidirectional enhancement operator.

A simple highpass filter can be achieved by subtracting this mask from the identity operator:

$$\begin{array}{ccc} 0 & -1 & 0 \\ -1 & 5 & -1 \\ 0 & -1 & 0 \end{array} = \begin{bmatrix} 0 & 0 & 0 \\ 0 & 1 & 0 \\ 0 & 0 & 0 \end{bmatrix} - \begin{bmatrix} 0 & 1 & 0 \\ 1 & -4 & 1 \\ 0 & 1 & 0 \end{bmatrix}$$

This is the same mask used as an example in unsharp masking enhancement.

Another commonly used method for mask design is frequency sampling.

For a given picture, its frequency response is specified. Thus in this problem the filter's frequency response of interest is known from other considerations.

The algorithm to derive the spatial domain mask is listed below.

- (1) Define the ideal filter with the desired magnitude response and phase response in frequency domain, $H(u,v)$
- (2) Take the inverse DFT (IDFT) back to spatial domain to get $h(x,y)$
- (3) Multiply $h(x,y)$ with a chosen window to truncate the filter to the desired length: $f'(x,y) = h(x,y) * w(x,y)$

In step (2), in order to reduce aliasing, it is necessary to keep $h(x,y)$ much longer than $f'(x,y)$. This procedure usually does not give the desired filter response because of this aliasing in the spatial domain. But an iterative method based on a criterion of the minimum of least square error of $(H(u,v) - H'(u,v))^2$ can improve the desired filter (Oppenheim, 1975). The true frequency response of this filter can be viewed by amply zero padding $h'(x,y)$ and taking the DFT. ($h'(x,y)$ is the derived mask and $H'(u,v)$ is the DFT of $h'(x,y)$)

My study is in homomorphic image enhancement, image restoration and phase-only image processing. Especially, phase-only image processing has been mostly neglected in the digital image processing literatures. But phase information does play a very important role in image processing. Due to the nature of images, a lot of processing techniques may be improved or developed by the consideration of phase-only processing. These three topics are presented in the following three chapters. Each chapter includes background information, theory, algorithms, and examples.

CHAPTER II

HOMOMORPHIC IMAGE ENHANCEMENT

Introduction

(a) **Image scatter model.**—We see objects because they emit or scatter the light into our eyes to form an image by the psychophysical system. A digitally recorded picture is formed in the same way by the detector. Most objects do not emit light by themselves, but scatter the light. The scatter situation is of great interest in image processing. Figure 2-1 is the common and simple model of an imaging system (Cohen, 1993): I is the illumination or incident light, f is the scattered light, N is the normal which is perpendicular to the unit area dA of object P at (x,y) , illumination angle θ_i and scattered angle θ_r are the angles between I and N , and R and N respectively, ϕ_i and ϕ_r are the slopes of the projections of I and R onto the tangent plane at $P(x,y)$. θ_i and ϕ_i determine the illumination direction, and θ_r and ϕ_r determine the scatter direction. Let's define a scatter function $R(x,y)$ as the ratio of total amount of the scattered light over the total amount of the incident light,

$$R(x,y) = \frac{\int f(x,y,\lambda) S(\lambda) d\lambda}{\int I(x,y,\lambda) d\lambda}$$

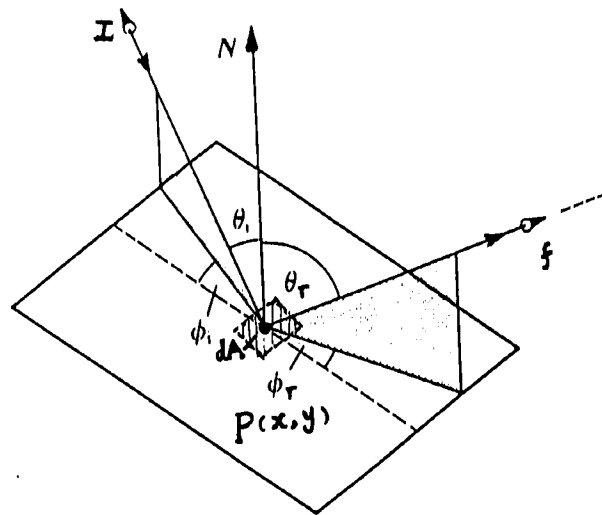


Fig. 2-1. Image scatter model

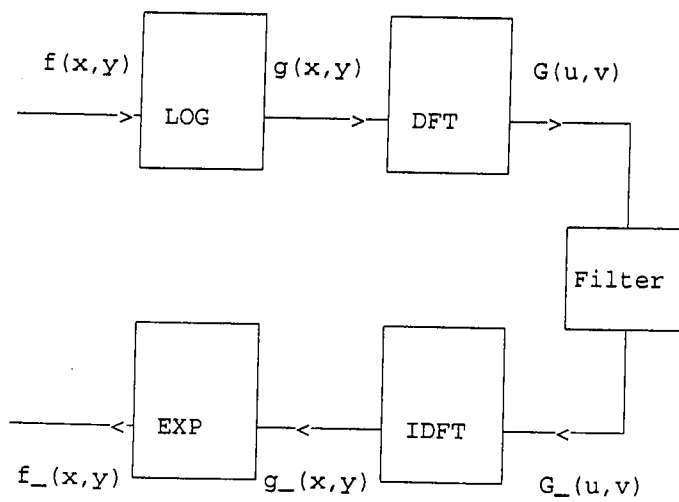


Fig. 2-2. Diagram of homomorphic image processing

where λ is the wavelength of light and the model may be simplified to be wavelength independent. $S(\lambda)$ is the sensitivity of the detector and can be taken as unity (i.e. one) in this study. It has been proved that the power per unit solid angle in the direction of the light ray is the same as the power per unit projected area. Thus,

$$R(x, y) = \frac{f(x, y) \cos \theta_r dA}{I(x, y) \cos \theta_i dA}$$

If the light source is infinitely far away, the incident lamp is assumed to be parallel, and if the detector or eye subtends a rather narrow angle, the scattered light is parallel as well. Meanwhile if the detector or the eye is assumed to be far away from the object, the surface of the object may be regarded as flat. Thus the scatter function $R(x, y)$ doesn't depend on any angle anymore and the scatter model turns into a rough reflection model, which is

$$f(x, y) = I(x, y) R(x, y)$$

$f(x, y)$ can be considered as the intensity of a pixel inside a recorded image corresponding to the object at $P(x, y)$. In the scattered radiation imaging system, the illumination part $I(x, y)$ changes very slowly in the picture, and is largely related to the diffuse and smooth area of pictures. The illumination contributes most to the dynamic range and the low frequency. The scattered component $R(x, y)$ changes very rapidly; it contains the edge information of pictures. The scattered component has high frequency content that represents

the edge information. The contrast enhancement may result in the edge enhancement, and may possibly be applied to edge detection.

(b) Homomorphic image processing.—The question then is how to take advantage of the representation of a picture with these two components, $I(x,y)$ the low frequency part, and $R(x,y)$, the high frequency part. If simply applying filter $h(x,y)$ to the picture $f(x,y)$, it will affect both $I(x,y)$ and $R(x,y)$. Our attempt is to separate the different frequency components and apply the appropriate filter to enhance or eliminate a certain range of frequency of interest. Homomorphic processing provides a transformation, thus maps the operation in one space into another space where the operation may be easily performed. Taking the natural logarithm of $f(x,y)$, gives

$$g(x,y) = \ln f(x,y) = \ln I(x,y) + \ln R(x,y)$$

filtering $\ln f(x,y)$ with respect to the frequency component of interest, then,

$$g'(x,y) = h(x,y) ** g(x,y),$$

where $**$ is the convolution operation. The filtered picture can be retrieved by taking the exponential of $g'(x,y)$, thus

$$f'(x,y) = e^{g'(x,y)}$$

The homomorphic filter is non-linear and thus may satisfy a human's non-linear psychophysical model. Our next intention is to discuss the filter for contrast enhancement and dynamic range compression.

In the photography process, we may select the different materials and

control the process time in order to achieve a large dynamic range which provides higher resolution and more information. One simple way to change the dynamic range of an image is to raise each pixel strength to a power γ :

$$f'(x,y) = f^\gamma(x,y)$$

The larger γ (always greater than 1.0), the larger the dynamic range, and vice versa. The increase of dynamic range may help contrast enhancement. But in some situations, a reduction in dynamic range is desired. For example, the resolution of a detector is 16-bits, but the display system can handle only 8-bits. The extra 8-bits are overhead. The larger dynamic range requires a larger storage space and longer transmit time. The dynamic range compression is a solution. If γ is chosen below 1.0, then the dynamic range is reduced.

The contrast enhancement is to boost the high frequency component $R(x,y)$. A high-pass boost or high frequency emphasis filter is desired. With many lowpass filters, such as Butterworth and Chebyshev lowpass filters, a highpass filter can be achieved by

$$f_H(x,y) = 1.0 - f_L(x,y)$$

Multiplying with an emphasis factor 'a',

$$a f_H(x,y) = a [1.0 - f_L(x,y)]$$

A constant or a low pass filter $f_L(x,y)$ is added as an offset to conserve the low frequency information, since a constant may be viewed as an all pass filter and

a lowpass filter will not attenuate the low frequency information. The final filter is written as (Alexander, 1986),

$$f_H(x,y) = a [1.0 - f_L(x,y)] + 1.0$$

or

$$f_H(x,y) = a [1.0 - f_L(x,y)] + f_L(x,y)$$

If we would like to have contrast enhancement and dynamic range compression at the same time, it is easily implemented by adjusting the offset of high emphasis filter to begin at γ_i , since γ_i smaller than 1.0 helps to compress the dynamic range, and the emphasis factor is chosen as γ_r , which is normally greater than 1.0 and helps to increase the contrast. Thus the result of picture will be,

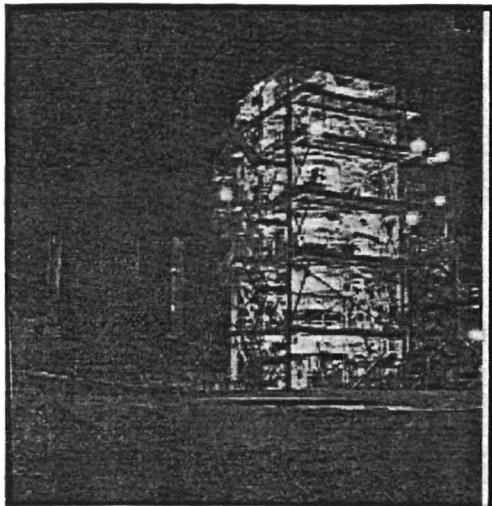
$$f'(x,y) = I^r(x,y) + R^r(x,y),$$

and the selected filter is

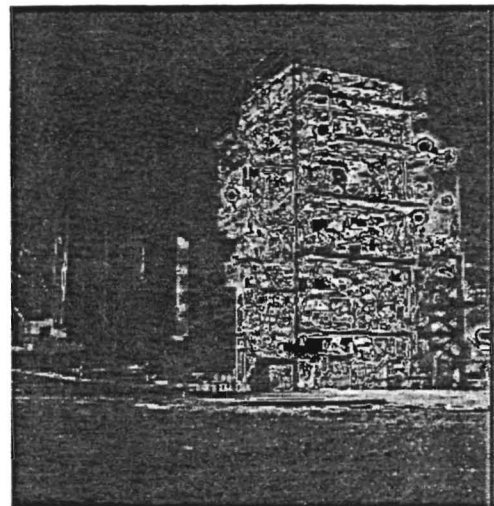
$$f_H(x,y) = \gamma_r [1.0 - f_L(x,y)] + \gamma_i$$

Experiment

The homomorphic image processing is diagramed in Figure 2-2. Following this diagram, a complete program is easily implemented. The results are shown in Figure 2-3. We can see the different values of γ controlling contrast enhancement ($\gamma > 1$) in Figure 2-3b. On the other hand, dynamic range



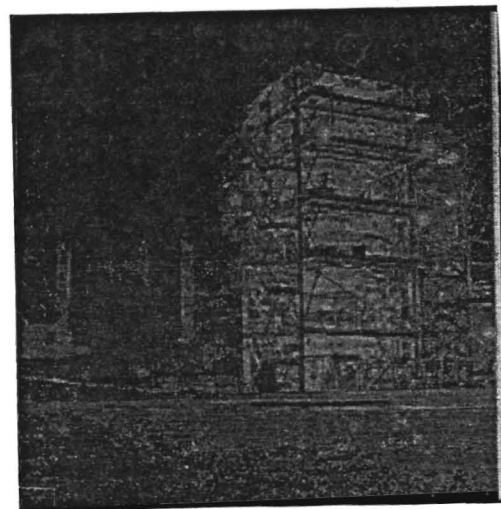
(a) The original picture 'TOWER'



(b) The picture with dynamic range increased by a constant homomorphic filter $h(x,y) = 1.18$ ($\gamma = 1.18$)

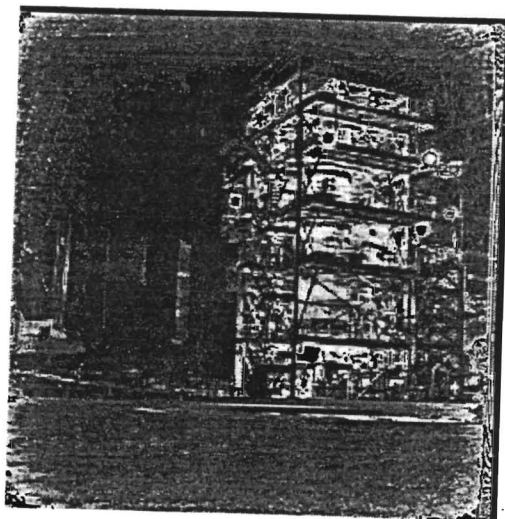


(c) The picture with contrast enhancement by a high emphasis filter with a factor $a = 1.65$

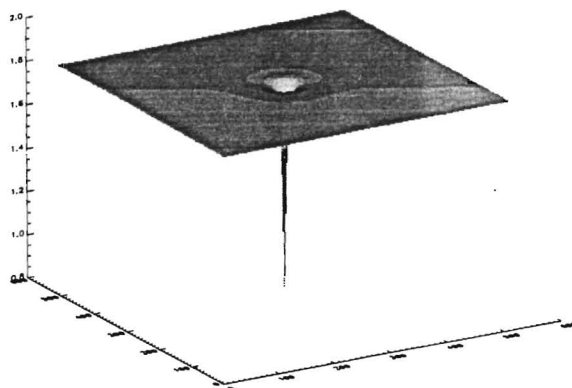


(d) The picture with dynamic range compression by a constant homomorphic filter $h(x,y) = 0.9$ ($\gamma = 0.9$)

Fig. 2-3. Homomorphic image processing: contrast enhancement and dynamic control



- (e) The picture with both contrast enhancement and dynamic range compression by a highpass filter with $\gamma_r = 1.65$ and $\gamma_i = 0.85$



- (f) The magnitude frequency response of the filter to handle both contrast enhancement and dynamic range compression

Fig. 2-3. (Continued)

compression ($\gamma < 1$) is shown in Figure 2-3d. The high emphasis filter enhances the contrast, while it keeps the low frequency component in Figure 2-3c. The contrast enhancement and dynamic range compression filter's spectrum is shown in Figure 2-3f and the picture processed by this filter is shown in Figure 2-3e with good results.

Conclusion

Under the simple scattering model, an image consists of both low frequency illumination and high frequency scatter components. A relatively simple non-linear homomorphic filter provides a good solution for contrast enhancement, dynamic range compression, or both simultaneously.

CHAPTER III

IMAGE RESTORATION

Introduction to image restoration

The ultimate goal of image restoration is to recover the original image from the degraded or noise-buried images with some a priori or a posterior knowledge. This kind of research began in the late of 1960s and a lot of advances have been made since (Sezan et al.,1990). The framework of image restoration includes modeling, identification and restoration.

There are two kinds of models involved: the observation model and the image model. The observation model tends to establish a mathematical model of forming a degraded image, for example, one of the models looks like

$$g(x,y) = S [h(x,y) ** f(x,y) + n(x,y)]$$

where $S[\dots]$ is a function of detector's effect, $f(x,y)$ is the original picture, $g(x,y)$ is the degraded picture, $h(x,y)$ is the degraded filter or point spread function (PSF), and $n(x,y)$ is the noise. The observation model tries to figure out the correct effect of an imaging system from detectors, degraded filters, and noise. The image model addresses of a 2-D image as a 2-D deterministic sequences or a random field. It is worth pointing out the definition of the random field, since it is a widely used model, and is convenient for some

restorations. A family of random variables $f(\mathbf{r}, \omega_i)$ is defined as a random field. It is the function of \mathbf{r} or ω_i with respect to each other, where \mathbf{r} is a set of discrete points or numbers to generate a family of random variables and the outcome ω_i is the i th member of the class. In a 2-D picture, \mathbf{r} may represent the vector position in x-y plane, say (x, y) , and ω_i may be the i th picture in a class of the collected pictures. It is easy to see for a given ω_i or a certain picture, $f(\mathbf{r}, \omega_i)$ can be regarded as a 2-D function or a picture in the x-y plane. Then the picture is assumed to have a certain probability distribution function (PDF) for the random variable $f(\mathbf{r}, \omega_i)$ at the point \mathbf{r} or (x, y) in the x-y plane, which is denoted as

$$P_f(\mathbf{r}) = \phi \{f(\mathbf{r}, \omega_i)\}$$

where ϕ is the probability of event $f(\mathbf{r}, \omega_i)$. Then stochastic processes and statistical techniques can be applied to image processing.

Identification is a procedure to identify the above models' parameters, or a priori and a posteriori knowledge of the models. For example, the identification of the observation model may involve determining what the type of blur is, motion blur or defocus blur, or what the kind of noise, white noise or colored noise. A priori information is an existent knowledge, such as the degradation by a zero phase degraded filter, so that it can be assumed that the degraded picture has the same phase spectrum as that of the original picture. A posteriori information is the knowledge computed from the existent

information, such as the estimated variance of the noise from a degraded picture. A priori or a posteriori knowledge are always necessary in image restoration. The more such knowledge, the more precise the model, and finally the better the restoration.

The final step is restoration. It requires restoration filter design and then inverse filtering. There are hundreds of restoration algorithms available. They may be classified by:

- (1) linear vs. non-linear
- (2) iterative vs. non-iterative
- (3) deterministic vs. stochastic

My study in this chapter uses Fourier computing to implement the basic restoration algorithms. First, let us begin with a certain imaging model. In the above observation model's example, because of the linear character of today's charge-coupled devices (CCD), which are much better than chemical films, the detector's non-linear effect $S[. . .]$ may be eliminated. The degraded filter $h(x,y)$ can be then assumed to be a LSI operator and the noise $n(x,y)$ is assumed to be signal independent, additive noise. Then the observation model will be

$$g(x,y) = h(x,y) ** f(x,y) + n(x,y)$$

If a restoration filter $m(x,y)$ exists, then the restored picture $f'(x,y)$ will be

$$f'(x,y) = m(x,y) ** g(x,y)$$

It should be noted that there is no unique solution in image restoration due to the nature of the inverse problem. The most common problems with image restoration are: singularities, non-uniqueness, and ill-conditioning.

Sometimes the restoration filter $m(x,y)$ may not exist. This is the problem of singularities. Karl (1989) shows a simple example for which, with a known short sequence and the known final convolution result, it may be unable to recover the long sequence due to lack of the sufficient information.

Even though the restoration filter $m(x,y)$ exists, there may be more than one solution of $m(x,y)$. This is the problem of non-uniqueness.

The last problem of ill-conditioning is that the restored picture's error or the difference between the original picture and the restored picture is large and cannot be negligible. The result may be that the restored picture is worse than the degraded picture in some point of view, such as the signal to noise ratio (SNR).

Since the Fourier computing is employed here for image restoration, it is necessary to discuss the approximation required in Fourier computing of digital signals. A 1-D LSI operator $h(t)$ may be expressed in a Toeplitz matrix:

$$\begin{pmatrix} h_1 & 0 & 0 \\ h_2 & h_1 & 0 \\ h_3 & h_2 & h_1 \\ h_4 & h_3 & h_2 \\ h_5 & h_4 & h_3 \end{pmatrix}$$

As we know, with enough zero padding (at least 2:1 zero padding over the long sequence), the overlap between two linear convolution sequences is avoidable, and the linear convolution can then be treated with the circular convolution. Our attempt here is to construct the circulant matrix (which will be defined next) from the Toeplitz matrix, which may be carried out by the discrete Fourier transform(DFT). The circulant matrix after the zero padding over Toeplitz matrix becomes

$$\begin{pmatrix} h_1 & 0 & 0 & 0 & 0 & 0 \\ h_2 & h_1 & 0 & 0 & 0 & 0 \\ h_3 & h_2 & h_1 & 0 & 0 & 0 \\ 0 & h_3 & h_2 & h_1 & 0 & 0 \\ 0 & 0 & h_3 & h_2 & h_1 & 0 \\ 0 & 0 & 0 & h_3 & h_2 & h_1 \end{pmatrix}$$

In a circulant matrix, each row is the right shift of the row above and the first row is the right shift of the last row. For an image or 2-D matrix, zero padding adds zero in the same positions as the above Toeplitz matrix of h : the upper right corner and lower left corner. In the circular framework LSI convolutions can be accomplished by the DFT. The periodic sequence is assumed outside the DFT window. But for some image models, zero is assumed outside the image. This significant character of the DFT may cause artifacts in image restoration. Some restored pictures may have the obvious crossing bars (Andrew and Hunt, 1977). Generally, the edge effect of DFT

computing is unavoidable in image restoration. Some methods have been proposed to solve this problem, for example, using a convolution operation in the time domain instead of a Fourier transform in the frequency domain, or using windowing to reduce the edge effect.

It is easy to apply the DFT to image processing under the random field assumption. A picture may be represented as $f(\mathbf{r})$. Its expected value may be noted as $E\{f(\mathbf{r})\}$, and its autocorrelation is $R(\mathbf{r}_1, \mathbf{r}_2) = E\{f(\mathbf{r}_1) f(\mathbf{r}_2)\}$, and its autocovariance is $C(\mathbf{r}_1, \mathbf{r}_2) = E\{[f(\mathbf{r}_1) - u(\mathbf{r}_1)][f(\mathbf{r}_2) - u(\mathbf{r}_2)]\}$. If the mean values of $u(\mathbf{r}_1)$ and $u(\mathbf{r}_2)$ are zero, then the autocovariance becomes the autocorrelation: $R(\mathbf{r}_1, \mathbf{r}_2) = C(\mathbf{r}_1, \mathbf{r}_2)$. One very important property of the Fourier transform is that the Fourier transform (\mathcal{F}) of a function's autocorrelation is its power spectrum. That is, $|F|^2 = \mathcal{F}\{R(\mathbf{r}_1, \mathbf{r}_2)\} = \mathcal{F}\{C(\mathbf{r}_1, \mathbf{r}_2)\}$. This expression will be directly applied in the coming sections.

Before closing this section, let me quote from Sezan and Tekalp (1990) stress that the current difficulties in image restoration stem from a lack of

- (1) fast and reliable blur identification methods,
- (2) general efficient algorithms for the identification and restoration of space variant (SV) blur,
- (3) the presence of artifacts in restored image.

It is hoped that there will be breakthroughs in these area in the near future.

Inverse filter

(a) Introduction.—The observation model of interest in the previous section is

$$g(x,y) = h(x,y) ** f(x,y) + n(x,y)$$

Its Fourier transform is

$$G(u,v) = H(u,v) F(u,v) + N(u,v)$$

If there exists a restoration filter $H^{-1}(u,v)$, then multiplying it on the both sides gives

$$\begin{aligned} H^{-1}(u,v) G(u,v) &= H^{-1}(u,v) H(u,v) F(u,v) + H^{-1}(u,v) N(u,v) \\ &= F(u,v) + H^{-1}(u,v) N(u,v) \end{aligned}$$

So the exact restored picture will be

$$f'(x,y) = \mathcal{F}^{-1}\{F(u,v)\} = \mathcal{F}^{-1}\{H^{-1}(u,v) G(u,v) - H^{-1}(u,v) N(u,v)\} \quad (3.1)$$

where \mathcal{F}^{-1} is the inverse Fourier transform, and $H^{-1}(u,v)$ is the inverse filter.

The above derivation is based on the Fourier transform. Given the degraded filter $H(u,v)$ and the noise $N(u,v)$, the exact restoration may be found. But in practical applications, these two terms need to be estimated.

There is another derivation based on the least square of the noise term, which may bring a deeper understanding to the inverse filter. The whole approach tends to find a smooth image with a lower noise variance and thus the noise variance is taken as a criterion.

$$n(x,y) = g(x,y) - h(x,y) ** f(x,y)$$

for a convenient notation, let H_T be the Toeplitz matrix and write,

$$n = g - H_T f$$

The noise's variance can be computed from the multiplication of the noise matrix with its transpose. Then

$$\delta_n^2 = n n^t = (g - H_T f) (g - H_T f)^t$$

The minimum of variance is found by differentiating with respect to the desired restored picture f' . Giving

$$\frac{\partial}{\partial f'} [(g - H_T f) (g - H_T f)^t] = 0$$

Then

$$H_T^t f' - H_T^t = g^t H_T$$

Taking the transpose on both sides and retrieving f' gives,

$$f' = (H_T H_T^t)^{-1} g H_T^t = H_T^{-1} g = H_T^{-1} (H_T f + n) = f + H_T^{-1} n \quad (3.2)$$

From equations (3.1) and (3.2), we can see that with the absence of noise, the image can be exactly recovered. But with the presence of noise, $\{H^{-1} n\}$ will

contribute to the new noise. This implies ill-conditioning in the inverse filter.

Let us discuss the singularities and the ill-conditioning problem next. When $H^{-1}(u,v)$ doesn't exist, the singularities problem arises. If $H(u,v)$ has at least one zero eigenvalue, it will result in a non-existent $H^{-1}(u,v)$. Most likely, a number of eigenvalues of $H(u,v)$ may be zero. One way to alleviate $H(u,v)$

from its zero component is to add a small constant in frequency domain. This is called whitening because the spectrum of white noise is constant and flat. The ill-conditioning situation in the inverse filter may be serious. The error from the inverse filtering on the noise term such as $H^{-1}(u,v) N(u,v)$ or $H^{-1}_T n$ will be numerous if H^{-1} or H^{-1}_T is far greater than 1.0. According to Parseval's theorem, which is

$$\int_{-\infty}^{\infty} \int_{-\infty}^{\infty} |f(x, y)|^2 dx dy = \int_{-\infty}^{\infty} \int_{-\infty}^{\infty} |F(u, v)|^2 du dv \quad (3.3)$$

the noise will have the same power on both spatial and frequency domain. A criterion for noise image situation is SNR, which is defined as

$$SNR = \frac{\delta_f^2}{\delta_n^2}$$

where δ_f^2 and δ_n^2 are the variances of image and noise respectively. If it is assumed that the restored picture f' has the same power as the original picture f , that is $\delta_{f'}^2 = \delta_f^2$, and if the new variance of noise $\delta_{n'}^2$ calculated from $\{H^{-1}(u,v) N(u,v)\}$ is greater than previous $\delta_{n'}^2$, then the recovered picture may be worse than the degraded picture from the point of view of SNR.

A very common white noise degraded picture's power spectrum is illustrated in Figure 3-1. The noise spectrum is rather flat and occupies almost the whole spectrum. The picture's spectrum seems to be added on the tail of

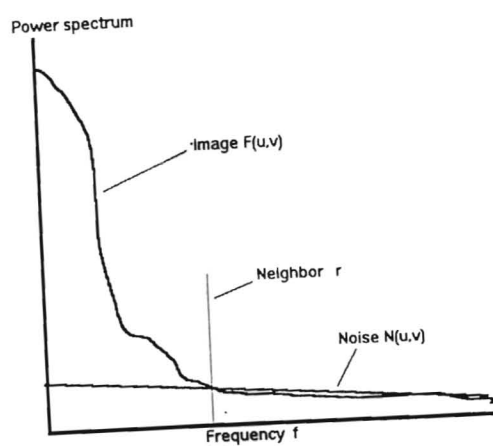
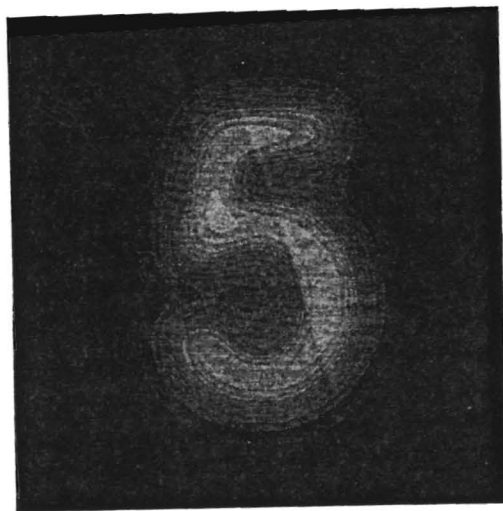


Fig. 3-1. The power spectrum of a noise image



(a) The original picture '5'

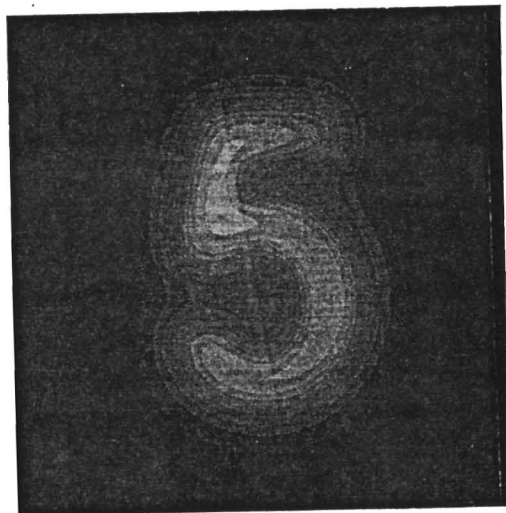


(b) The picture degraded by a Butterworth lowpass filter without noise

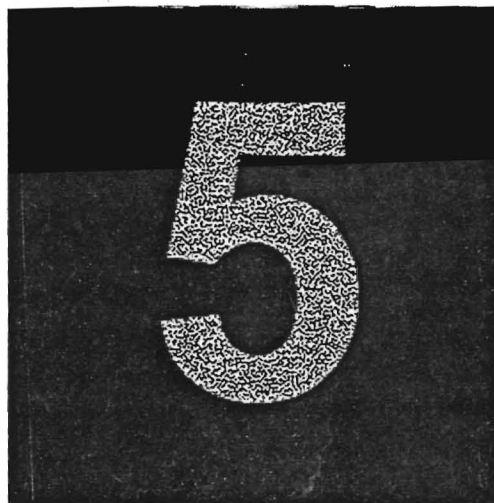


(c) The recovered picture of (b)

Fig. 3-2. Examples of the inverse filter



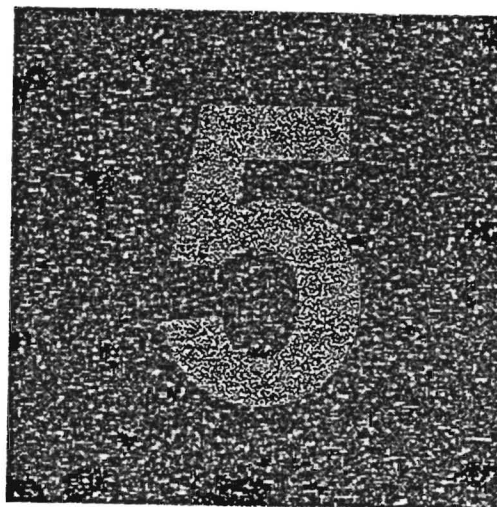
(d) The picture degraded by both a Butterworth lowpass filter and the high SNR additive noise



(e) The recovered picture of (d)

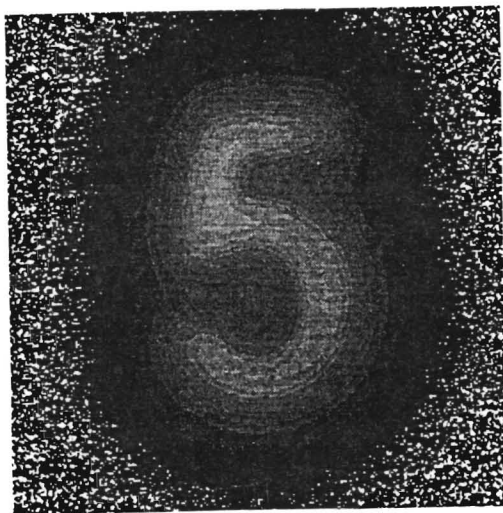


(f) The picture degraded by both a Butterworth lowpass filter and the low SNR additive noise



(g) The recovered picture of (f)

Fig. 3-2. (Continued)



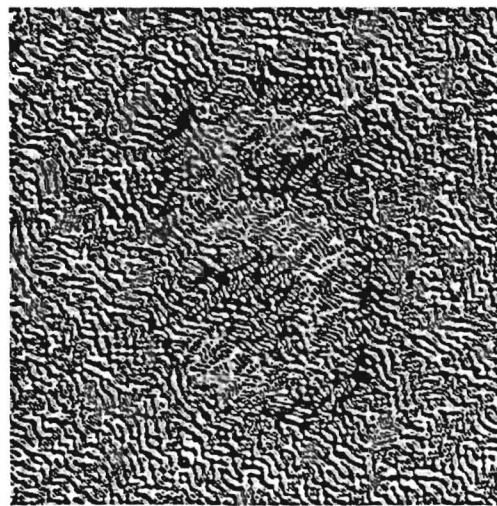
(h) The picture degraded by both a Butterworth lowpass filter and the very low SNR additive noise



(i) The picture of (h) recovered by the inverse filter applied to a small neighborhood range r



(j) The picture of (h) recovered by the inverse filter applied to a medium neighborhood range r



(k) The picture of (h) recovered by the inverse filter applied to a large neighborhood range r

Fig. 3-2. (Continued)

the noise and it changes rapidly within a certain range r of (u,v) , say $u^2 + v^2 \leq r^2$. The ill-conditioning is due to a large $H^{-1}(u,v)$ value affecting much on those noise components beyond the range r . One efficient way to solve this problem is to only allow $H^{-1}(u,v)$ filtering the signal's terms within a certain neighborhood range r and set $H^{-1}(u,v)$ to be a unit elsewhere. Then the improved inverse filter is

$$H^{-1}(u,v) = \begin{cases} 1.0 / H(u,v) & \text{for } u^2 + v^2 \leq r^2 \\ 1.0 & \text{for } u^2 + v^2 > r^2 \end{cases}$$

(b) Experiment.—The algorithm to implement the inverse filter by Fourier computing is given below.

- (1) With at least 2:1 zero padding to compute Fourier transform of the degraded picture $G(u,v)$ from $g(x,y)$
- (2) With enough zero padding to make the same length of degraded filter and make it symmetric to eliminate the phase shift problem, then compute Fourier transform of the degraded filter $H(u,v)$ from $h(x,y)$
- (3) Only compute the inverse filter within the range of $u^2 + v^2 \leq r^2$ as $H^{-1}(u,v) = 1.0/H(u,v)$ and set it to be 1.0 elsewhere as $H^{-1}(u,v) = 1.0$
- (4) Filter the degraded picture: $F(u,v) = G(u,v) H^{-1}(u,v)$
- (5) Compute the restored picture from the inverse Fourier transform of $F(u,v)$.

A small number such as $1E^{-30}$ is added to prevent the problem of dividing by zero in computing the inverse filter.

The test results are shown in Figure 3-2. Perfect restoration is made where there is no noise present (Figure 3-2c). Comparing the results of a high SNR (Figure 3-2e) with those of a low SNR (Figure 3-2g), we see the inverse filter is very noise sensitive and the ill-conditioning is very serious. What's more, within a small neighborhood range r , the restoration is highly intelligible, but in a large neighborhood range r , the restoration will be difficult to identify due to the ill-conditioning from the inverse filtering on the noise term (Figure 3-2k). The results confirm the spectrum distribution of the noise picture.

(c) **Conclusion.**—Inverse filter is the inverse of the degraded filter and also a least square filter. The restored picture can be exactly recovered from the inverse filter without noise or in a very high SNR condition. The small neighborhood range helps to eliminate the ill-conditioning. Generally the inverse filter is bad in noise immunity.

Wiener filter

(a) **Introduction.**—In the previous section, the inverse filter was derived by the least square of the noise variance. It is a rather loose criterion because it doesn't touch the noise and image models at all. This filter is very noise sensitivity and does little to improve the SNR. This section is going to introduce a more vigorous criterion: minimum mean square error (MMSE),

which will result in a rather robust Wiener filter. Before using the MMSE criterion, let us introduce a simple derivation of Wiener filter which actually does satisfy the MMSE criterion, although it is not obvious from the presentation.

Using the same observation model as in the previous sections,

$$g(x,y) = h(x,y) ** f(x,y) + n(x,y)$$

If there exists a restoration filter $m(x,y)$, assume the picture can be exactly recovered from,

$$g(x,y) ** m(x,y) = f(x,y)$$

For better notation, writing in brief,

$$g ** m = f$$

Convolving the complex conjugate of the reverse of g on both sides gives

$$g_-^* ** g ** m = g_-^* ** f$$

Defining the autocorrelation and crosscorrelation as

$$C_{g,f} = g^* \otimes f = g_-^* ** f$$

and

$$\Phi_{g,g} = f^* \otimes f = f_-^* ** f$$

Thus

$$m = \frac{C_{g,f}}{\Phi_{g,g}} = \frac{g^* \otimes f}{g^* \otimes g}$$

Since

$$g^* \otimes f = (h ** f + n)^* \otimes f = h^* ** f^* \otimes f + n^* \otimes f$$

and

$$\begin{aligned} g^* \otimes g &= (h ** f + n)^* \otimes (h ** f + n) \\ &= h^* ** f^* \otimes h ** f + h^* ** f^* \otimes n + n^* \otimes h ** f + n^* \otimes n \\ &= h^* \otimes h ** f^* \otimes f + h^* ** f^* \otimes n + h ** n^* \otimes f + n^* \otimes n \end{aligned}$$

Because it is assumed that there is no any correlation between the signal and the noise,

$$n^* \otimes f = 0 \text{ and } f^* \otimes n = 0$$

The final result of m is

$$m = \frac{h^* ** f^* \otimes f}{f^* \otimes f ** h^* \otimes h + n^* \otimes n} = \frac{h^*}{\Phi_{h,h} + \frac{\Phi_{n,n}}{\Phi_{f,f}}} \quad (3.4)$$

Given the autocorrelation of the picture and the noise, and the knowledge of the degraded filter, the exact restoration may be found.

Let's go further to see that this result is the same as that from MMSE criterion.

Assume the restored picture is,

$$f'(x,y) = m(x,y) ** g(x,y)$$

Generally, a good restoration will be as close as possible to the original image.

An error between the restored picture and the original one is

$$e = f(x,y) - f'(x,y) = f(x,y) - m(x,y) ** g(x,y)$$

The error e may represent the random numbers, and the sum square error or the variance of zero mean may be represented as

$$\Sigma (e^2_i) = e e^t = \{f(x,y) - m(x,y) ** g(x,y)\} \{f(x,y) - m(x,y) ** g(x,y)\}^t$$

where t is the transpose of the corresponding matrix. For a convenient notation, assume that $m(x,y)$ and $h(x,y)$ are Toeplitz matrices M_T and H_T respectively, and write in,

$$\begin{aligned} \Sigma (e^2_i) &= \{(f - M_T g)\} \{(f - M_T g)\}^t \\ &= \{f - M_T (H_T f + n)\} \{f - M_T (H_T f + n)\}^t \end{aligned}$$

since,

$$f n^t = 0 \text{ and } n^t f = 0$$

The result would be

$$e e^t = f f^t - f f^t H_T^t M_T^t - M_T H_T f f^t + M_T H_T f f^t H_T^t M_T^t + M_T n n^t M_T^t$$

The minimum of variance is found by differentiating with respect to the desired filter M and forcing it to be zero,

$$\frac{\partial}{\partial M} [e e^t] = 0$$

or

$$-H_T f f^t + H_T f f^t H_T^t M_T^t + n n^t M_T^t = 0$$

Taking the transpose of both sides and retrieving M gives

$$M = \frac{(f^t f) H_T^t}{H_T f f^t H_T^t + n n^t}$$

All these Toeplitz matrices such as H_T , H_T^t , f , f^t , M_T , M_T^t , n , n^t may be used to construct the circulant matrices with sufficient zero padding on its upper right and lower left corner. As we know, the eigenvalue λ of a circulant matrix H_C is the Fourier transform of its cyclic sequence $h(j)$.

$$\lambda(k) = \sum_0^{N-1} c(j) e^{-j \frac{2\pi k j}{N}}$$

or

$$\lambda(k) = \text{DFT} \{c(j)\}$$

Let us define $e^{-j2\pi k j/N}$ as a matrix W . It is obvious that the inverse Fourier transform, that is $(1/N)e^{j2\pi k j/N}$, can be defined as the inverse matrix W^{-1} . If λ_d is the diagonal matrix of eigenvalues, then the circulant matrix H_C can be represented as

$$H_C = [W] \lambda_d [W^{-1}]$$

And this expression has the following properties,

$$H_C^t = [W] \lambda_d^* [W^{-1}]$$

$$H_{C1} + H_{C2} = [W] (\lambda_1 + \lambda_2) [W^{-1}]$$

and

$$C_{C1} C_{C2} = [W] (\lambda_1 \lambda_2) [W^{-1}]$$

(Please refer to the appendix for detail.) So, the restoration filter may be represented as

$$M_c = \frac{f_c' f_c H_c'}{H_c f_c' H_c' + n_c n_c'} = [W] \frac{\lambda_f^* \lambda_f \lambda_h^*}{\lambda_h \lambda_f \lambda_f^* \lambda_h^* + \lambda_n \lambda_n^*} [W^{-1}]$$

Multiplying $[W]$ on the both sides gives

$$M_c [W] = [W] \frac{\lambda_h^* \lambda_f^* \lambda_f}{\lambda_h^* \lambda_h \lambda_f^* \lambda_f + \lambda_n^* \lambda_n}$$

Since $[W]$ represents the Fourier transform matrix, $M_c [W]$ is the Fourier transform of the circulant matrix M_c . And because $H_c = [W] \lambda_d [W^{-1}]$ may be written as $H_c [W] = [W] \lambda_d$, the expression $[W] \lambda_d$ is the Fourier transform of the corresponding circulant matrix H_c as well. So the result in the frequency domain is

$$M(u, v) = \frac{H^* F^* F}{H^* H F^* F + N^* N} = \frac{H^*}{|H|^2 + \frac{|N|^2}{|F|^2}} \quad (3.5)$$

Equation 3.5 was first derived by Pratt using a slightly different approach (Levune, 1985), and the so-called Wiener filter is a special case of it at $H=1.0$. But we still would like to call the general form of this restoration filter Wiener filter.

Equations 3.4 and 3.5 are the same except that Equation 3.5 is in the frequency domain. This is also why the derivation of Equation 3.4 satisfies the MMSE criterion. Equation 3.4's derivation is rather simple and easily following than other derivation found in the literature.

The singularities problem will not exist in a Wiener filter, because of the power spectrum of SNR term in the denominators. The SNR term also helps to compress the ill-conditioning. But due to the simple stochastic models of the image and noise, it makes a Wiener filter not sufficient in some applications.

(b) Experiment.—The algorithm to implement Wiener filter is listed below,

- (1) With at least 2:1 zero padding to compute the Fourier transform of the degraded picture $G(u,v)$ from $g(x,y)$
- (2) With enough zero padding to make the same length of degraded filter and make it symmetric to be zero phase, then compute the Fourier transform of the degraded filter $H(u,v)$ from $h(x,y)$
- (3) Compute the power spectrum of the original picture from $f(x,y)$, which is assumed to be known
- (4) Compute the variance of the noise from $n(x,y)$, which is assumed to be known as well

- (5) Construct the restoration filter $M(u,v)$ in frequency domain as

Equation 3.5

- (6) Filter the degraded picture: $F'(u,v) = M(u,v) G(u,v)$

- (7) The restored picture is computed by the inverse Fourier transform of $F'(u,v)$

All the noise in our experiments is zero mean Gaussian noise which is generated in this way,

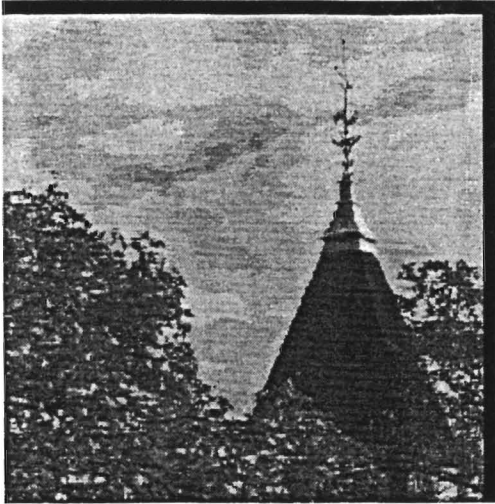
$$\text{noise} = \text{sqrt}(\text{variance}) * \text{randomn}(\text{seed})$$

'Randomn(seed)' is an IDL subroutine to generate the normal distribution random number and it is sampled from the unity distribution random number generated by a routine called 'randomu(seed)'. The relationship of these two random numbers is given below

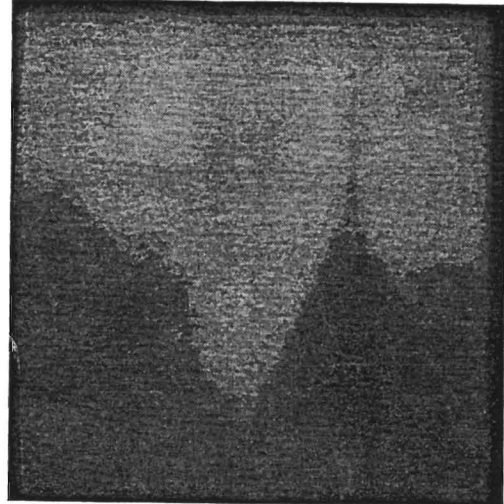
$$\text{randomn}(\text{seed}) = \{ \sum_{i=1}^{12} \text{randomu}(\text{seed}) \} - 6.0$$

Sampling is adding the unity distribution numbers 12 times and subtracting 6.0 to get zero mean, which is a result of the central limit theorem.

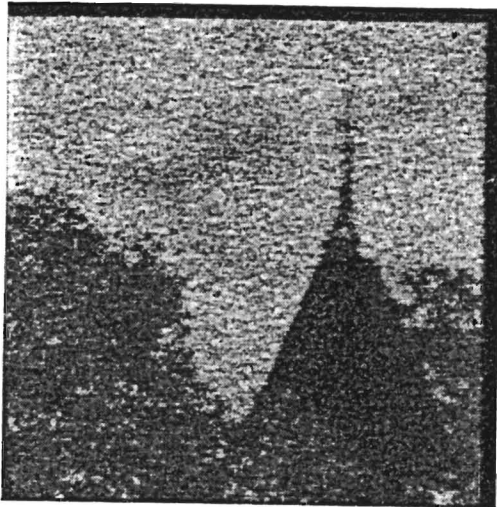
The results are shown in Figure 3-3. Compared to the inverse filter's case (Figure 3-3f), the Wiener filter is rather robust in noise environment (Figure 3-3e) in the same degradation situation. Even in the low SNR condition, say $\text{SNR} = 100$, the restored picture is still intelligible (Figure 3-3c).



(a) The original picture 'UWO'



(b) The picture degraded by both a Butterworth lowpass filter and additive noise (SNR = 100)

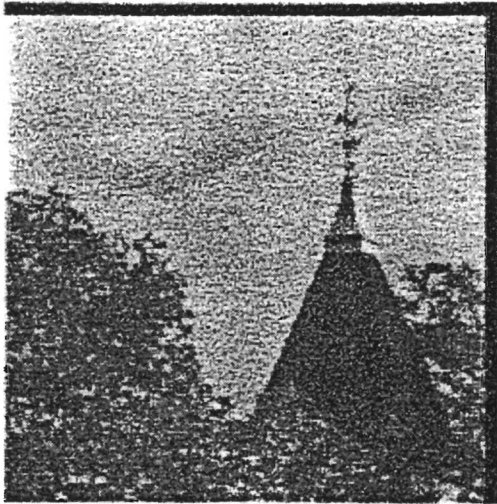


(c) The picture of (b) recovered by the Wiener filter



(d) The picture degraded by both a Butterworth lowpass filter and additive noise (SNR = 1000)

Fig. 3-3. Examples of the Wiener filter



(e) The picture of (d) recovered by the Wiener filter (f) The picture of (d) recovered by the inverse filter

Fig. 3-3. (Continued)

(c) **Conclusion.**—The Wiener filter is based on a better criterion than minimizing the noise variance, which was used in the inverse filter. The Wiener filter criterion is to obtain MMSE between the restored picture and the original picture. Wiener filter is a rather robust filter for noise immunity and the restored picture has remarkably been improved in SNR.

Magnitude-only inverse filter

(a) **Introduction.**—The criterion of Wiener filter is based on obtaining a restored picture which is the closest approximation to the original picture. This section is going to introduce another criterion which is based on the closest approximation of the power spectrum of the restored picture to that of the original one. Even though the criterion is looser than the Wiener filter, it will result in a magnitude-only filter of interest.

Using with the same observation model,

$$g(x,y) = h(x,y) ** f(x,y) + n(x,y)$$

if there exists the restored filter $m(x,y)$, the restored picture will be,

$$g(x,y) ** m(x,y) = f'(x,y)$$

Its Fourier transform is

$$G M = F'$$

According to Parseval's theorem (Equation 3.3), a time domain sequence will have the same power as that in the frequency domain, thus

$$|G|^2 |M|^2 = |F|^2$$

where $|G|^2$ and $|F|^2$ are the power spectra of the degraded picture and original picture respectively. So,

$$M = \sqrt{\frac{|F|^2}{|G|^2}}$$

It is obvious that $M(u,v)$ is a magnitude-only inverse filter. If the power spectrum of the original picture $|F|^2$ is known, the only thing left for the restoration filter is the power spectrum of the degraded picture $|G|^2$. This turns to a problem of power spectrum estimation of a degraded picture. A very common method is ensemble average, which is based on the ergodic assumption of an image. The average of picture $f(x,y)$ is presented as

$$E = \frac{1}{A} \int f(x, y) \, dx dy$$

where A is the area in averaging and $f(x,y)$ is a picture or a random field. If E is constant, then E is equal to the mean, and the random field is called ergodic with respect to the mean (Rosenfeld, 1982). If a collection of pictures is a random field, then the mean of the random field may be obtained from the spatial average over one of the collection pictures. This character will be applied in Chapter IV, which is to use the average magnitude of one of the collection pictures and the original phase spectrum of picture for image

synthesis. The other type of ergodic assumption of an image is ergodic with respect to the autocorrelation, which means the spatial average E is constant in the integration of the autocorrelation of $f(x,y)$ instead of the image $f(x,y)$. And E can be represented as

$$E = \frac{1}{A} \int \int f(x, y) f(x+a, y+b) dx dy$$

Also, the power spectrum of a collection of pictures in the random field can be obtained from the spatial average over the autocorrelation of one particular picture. Under this assumption, an ergodic picture may be partitioned into several segments, each of which can be used for power spectrum estimation of the complete picture. This partition averaging method is called ensemble averaging and it improves the SNR, since summing the noise data for N times, the signal grows N times as well, but the noise only grows \sqrt{N} times, thus the new SNR will grow $N/\sqrt{N} = \sqrt{N}$ times. But there is a significant tradeoff in ensemble averaging. Each segment is treated as a data window, which determines the frequency resolution. The smaller the segments, the more averaging operations, thus the better SNR, but the worse the frequency resolution. One improved method is allowing overlap among the segments which may not only maintain a certain size of data window, but also increase the averaging operations (Stearns, 1988). What percentage of the overlap is the best? There is no unique answer. It depends on the practical situation and is

determined by trial and error. Please note that inside an image, the pixels are only correlated within a small region. This means the overlap of segments may form a new data window. Meanwhile, if the distance between the pixels is beyond 20-30 pixels, there is no correlation at all. This implies that too much overlap may be useless. This filter is called ensemble average magnitude-only filter.

Another method to estimate the degraded picture's power spectrum directly begins with the definition of the power spectrum of a degraded picture, which is

$$|G|^2 = G^*(u,v) G(u,v) = (H F + N)^* (H F + N) = |H|^2 |F|^2 + |N|^2$$

Then the final restoration filter will be

$$M = \sqrt{\frac{1.0}{|H|^2 + \frac{|F|^2}{|N|^2}}}$$

It looks like a Wiener filter, but it is a magnitude-only filter. This filter is called Wiener magnitude-only filter and it requires the power spectrum of the degraded filter in computing, which is not known in some practical applications. In this situation, ensemble average magnitude-only plays a more important role.

(b) **Experiment.**—The algorithm to implement ensemble average is listed below:

- (1) Divide a degraded picture $g(x,y)$ into $N \times M$ segments and each segment containing $n \times m$ pixels
- (2) Compute the periodogram of each segment by Fourier computing,

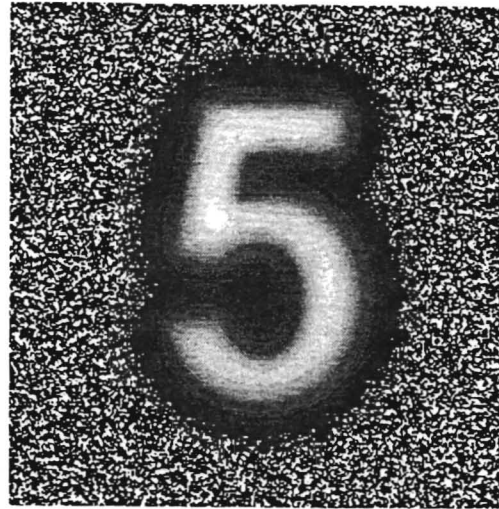
$$G(u,v) = (1.0/nm) [\text{DFT} \{ g(x,y) \}]$$
- (3) Sum every periodogram until all the segments have been processed,

$$|G|^2 = |G|^2 + (1.0/NM) G(u,v)$$
- (4) Compute the power spectrum of an original picture $|F|^2$, which is assumed to be known
- (5) Compute the power spectrum of the degraded picture $|G|^2$
- (6) Interpolate $|G|^2$ to the same length as $|G|^2$ by Fourier computing:
 transform $|G|^2$ into spatial domain, with enough zero padding, transform it back to frequency domain.
- (7) Form the magnitude-only inverse filter by $M(u,v) = \text{sqrt}(\Phi_f/\Phi_g)$
- (8) Filter the degraded picture by: $F'(u,v) = G(u,v) M(u,v)$
- (9) The restored picture is computed from the inverse Fourier transform of $F'(u,v)$.

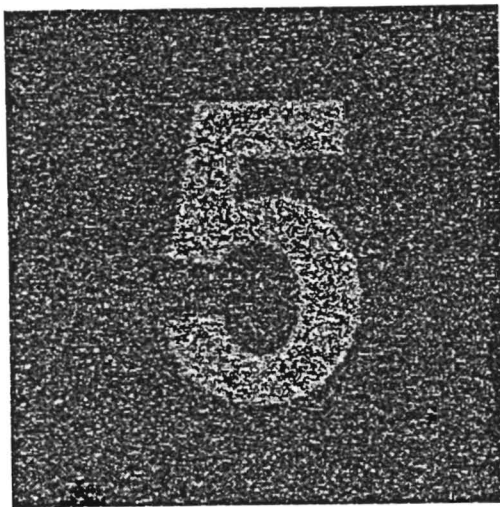
The results are shown in Figure 3-4 to Figure 3-6. Generally, the ensemble averaging has a better statistical resolution than Wiener magnitude-only filter, but there may be some loss in frequency resolution in the small window size



(a) The original picture '5'



(b) The picture degraded by both a Butterworth lowpass filter and the additive noise (SNR = 1000)



(c) The picture of (b) recovered by the Wiener magnitude-only filter

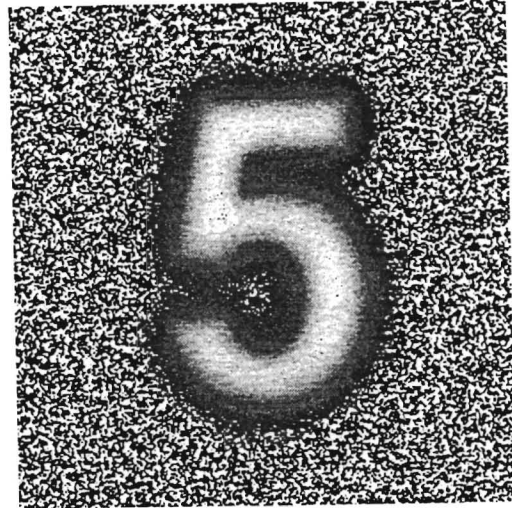


(d) The picture of (c) recovered by the ensemble averaging magnitude-only filter with window size = 64 and overlap = 32

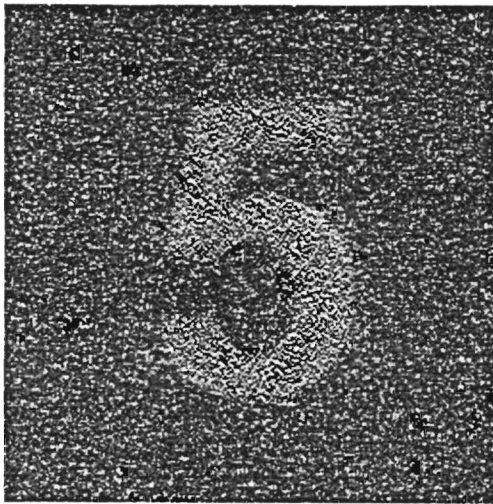
Fig. 3-4. Examples of magnitude-only inverse filter and ensemble averaging magnitude-only filter with SNR = 1000



(a) The original picture '5'



(b) The picture degraded by both a Butterworth lowpass filter and additive noise (SNR = 100)

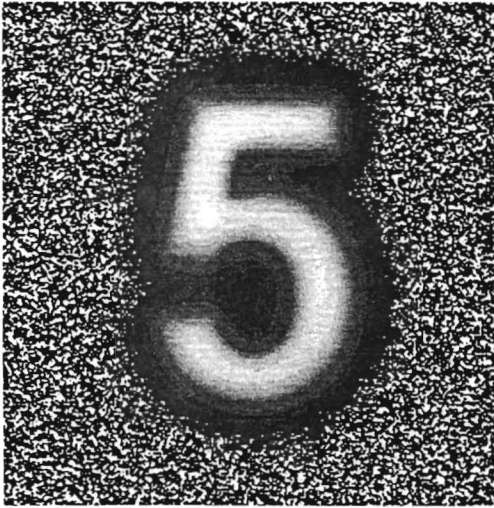


(c) The picture of (b) recovered by the Wiener magnitude-only filter



(d) The picture of (c) recovered by the ensemble averaging magnitude-only filter with window size = 64 and overlap = 32

Fig. 3-5. Examples of magnitude-only inverse filter and ensemble averaging magnitude-only filter with SNR = 100



(a) The picture degraded by both a Butterworth lowpass filter and the additive noise



(b) The picture of (a) recovered by the ensemble averaging magnitude-only filter with window size = 64 and overlap = 32



(c) The picture of (a) recovered by the ensemble averaging magnitude-only filter with window size = 128 and overlap = 32



(d) The picture of (a) recovered by the ensemble averaging magnitude-only filter with window size = 128 and overlap = 64

Fig. 3-6. Examples of ensemble averaging magnitude-only inverse filter with different window size and overlap length

(Figure 3-4c vs. Figure 3-4d and Figure 3-5c vs. Figure 3-5d). With a longer data window, the recovered picture has been improved in frequency resolution (Figure 3-6c vs. Figure 3-6d). The smaller the data window, the more addition operations, thus the improvement of statistical resolution (Figure 3-6b). And a proper window size and the length of overlap can improve both statistic and frequency resolution (Figure 3-6d). Meanwhile, with ensemble averaging some DFT artifacts occurs (Figure 3-6b), since ensemble averaging employs DFT to compute the periodogram of each segment.

(c) Conclusion.—Magnitude-only filter is assumed to be zero phase and will not change the phase spectrum. The ensemble average of the degraded picture estimation helps improve the SNR and with a proper window size and overlap length, a good restoration may be achieved. In the practical application, only a degraded picture and original picture's power spectrum are available, so the ensemble average will be very useful.

Summary

Three different restoration filters have been discussed. Recalling the definition of image restoration, we will see how important a priori and a posteriori knowledge are. All the derived filters are based on the different models. The table below is a summary of three types of filters .

Table 3-1. Summary of three types of restoration filters

	Inverse filter	Wiener filter	Magnitude-only filter
priori knowledge	$h(x,y)$	$h(x,y), \Phi_f, \Phi_n$	Φ_f
posteriori knowledge	no require	no require	Φ_g
criteria	$n n^t$	$(f-f') (f-f')^t$	$(f ^2 - f' ^2)(f ^2 - f' ^2)^t$
Noise immunity	bad	good	better
frequency resolution	unchanged	unchanged	decreased
statistical resolution	slightly improved	improved	much improved
singularities problem	yes	no	no
phase problem	no	no	yes

In the above table, $h(x,y)$ is the degraded filter, Φ_f , Φ_n and Φ_g are the power spectra of original picture, noise and degraded picture respectively, f' is the restored picture, magnitude-only filter refers to that of the ensemble averaging, and the criterion is taking the least square of the corresponding terms. Bad noise immunity may result in ill-conditioning in a low SNR situation.

Even though these three filters are derived from different constraints, they are related. Under some conditions, they can be changed to another form. For example, the Wiener filter is

$$M(u, v) = \frac{H^*}{|H|^2 + \frac{|M|^2}{|F|^2}}$$

if there is no noise present, $|N|^2 = 0$, then

$$M(u, v) = \frac{H^*}{|H|^2} = \frac{1.0}{H}$$

This is the inverse filter. In the condition of extremely low SNR, that is $|F|^2 \rightarrow 0$, then the Wiener filter will be $M(u, v) \rightarrow 0$ also. But for the magnitude-only inverse filter, the situation is different. Since $|G|^2 = |H(u, v)|^2 |F|^2 + |N|^2$, if $|F|^2 = 0$, then $|G|^2 = |N|^2$, thus the magnitude-only inverse filter will change from its original form

$$M(u, v) = \sqrt{\frac{\Phi_f}{\Phi_g}}$$

to

$$M(u, v) = \sqrt{\frac{\Phi_f}{\Phi_n}}$$

In this case, the magnitude-only inverse filter is proportional to the ratio of the power spectrum of the signal over the power spectrum of the SNR according to our definition. And this is why this kind of filter may be used in a very low SNR situation. If the degraded filter is a delta function, that is $H(u, v) = 1.0$, then the Wiener filter will become,

$$M(u, v) = \frac{1.0}{1.0 + \frac{|N|^2}{|F|^2}}$$

This is so-called Wiener filter which is derived by Wiener. It is the magnitude-only restoration filter as well. It can be successfully applied in the known SNR additive noise degradation.

Among these three filters, the ensemble average magnitude-only inverse filter requires the least a priori knowledge, except the power spectrum of the original picture. The Wiener filter requires more a priori knowledge and thus does a better job in most cases. However in some applications, the variance of the original picture is not available, and a variance estimation procedure is required. The iterative Wiener filter may be well applied in this case (Hillery et al., 1991). The iterative method begins with a variance of the degraded picture and treats it as the variance of the original picture. After filtering the degraded picture, it uses the variance of the restored picture as the variance of the new original picture again for the next step. The algorithm is listed below,

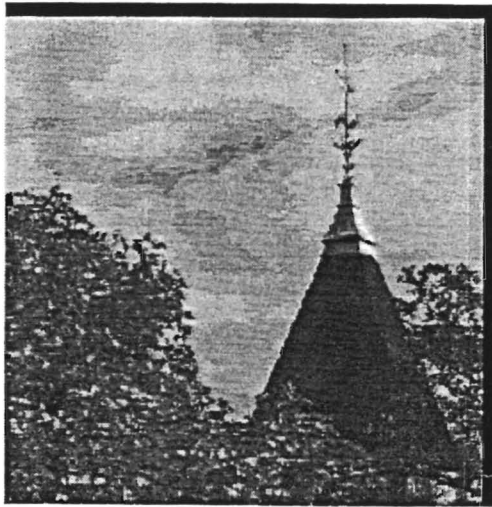
- (1) Compute the power spectrum of the degraded picture Φ_g and use it as the power spectrum of the original picture: $|G|^2 \rightarrow |\Phi|^2$
- (2) Compute the Fourier transform of the degraded picture: $G(u,v)$
- (3) Construct the Wiener filter from Equation 3.4: $M(u,v)$
- (4) Filter the degraded picture in the frequency domain: $F'(u,v) = G(u,v) M(u,v)$
- (5) Compute the restored picture $f'(x,y)$ from the inverse Fourier transform

of $F'(u,v)$

- (6) Compute the power spectrum of the restored picture $f'(x,y)$ and use it as the power spectrum of the original picture: $|F'|^2 \rightarrow |F|^2$
- (7) Compute the Fourier transform of a restored picture $G'(u,v)$, and take it as that of the new degraded picture: $G'(u,v) \rightarrow G(u,v)$
- (8) Goto (3) until the iterative condition is satisfied

The results are shown in Figure 3-7. We can see the restored picture after 10 iterations has been improved and results in more structured features in the tree and the black border of the picture (Figure 3-7d).

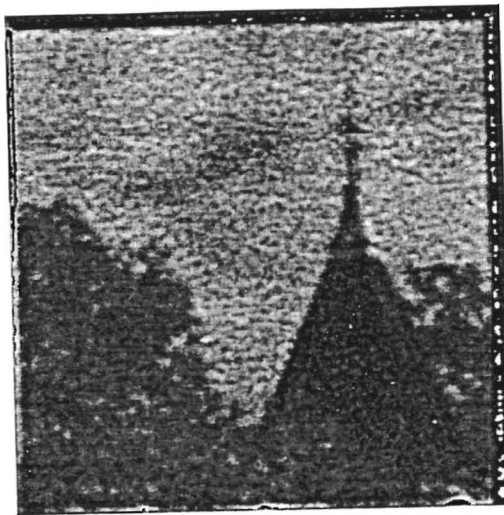
In the mathematical model point of view, Wiener filter is nearly perfect, but our non-linear visualization system does not show the enthusiasm to welcome it. Our visual psychology prefers some kind of noise and throws away some structured features. This is the reason some restored results from Wiener filter are not welcome. Here are some further discussions about the magnitude-only inverse filter. The criterion to derive the magnitude-only inverse filter is rather loose, as we will see in Chapter IV. In the common pictures, the power spectra of the common pictures look similar, especially in the low frequency region. But there is no doubt about the ability of ensemble averaging to reduce the variance of the degraded picture and to improve the SNR. A better proposal for ensemble average is windowing the data segments before computing their periodograms (Dudgeon, 1984). Finally, the magnitude-only



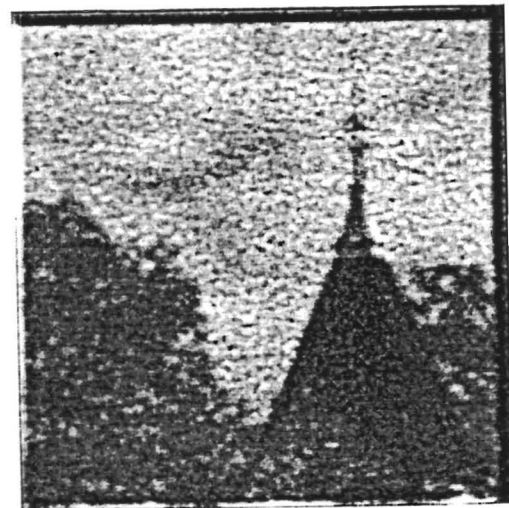
(a) The original picture 'UWO'



(b) The picture degraded by both a Butterworth lowpass filter and the additive noise



(c) The picture of (b) recovered by the iterative Wiener filter at the first time



(d) The picture of (b) recovered by the iterative Wiener filter after 10 times

Fig. 3-7. The example of the iterative Wiener filter

inverse filter assumes zero phase degradation, but in some applications, it may cause a problem. For example, the motion blur may be thought as a convolution between a picture and a box car. The Fourier transform of a box car is a sinc function and Gibbs phenomenon will exist in the frequency domain. The positive hump of the sinc function generates the zero phase, but its negative counterpart will give a 180-degree phase angle. Obviously, in this case, the magnitude-only filter cannot recover the correct phase spectrum and the wrong information may contribute to the edges of the picture.

CHAPTER IV

PHASE-ONLY IMAGE PROCESSING

The importance of phase in image synthesis

(a) Introduction.—As we have seen before, the Fourier transform plays an important role in image processing. The Fourier transform of an image $f(x,y)$ can be expressed as

$$F(u, v) = \int_{-\infty}^{+\infty} \int_{-\infty}^{+\infty} f(x, y) e^{-i2\pi (ux+vy)} dx dy$$

The inverse Fourier transform can be written as

$$f(x, y) = \int_{-\infty}^{+\infty} \int_{-\infty}^{+\infty} F(u, v) e^{i2\pi (ux+vy)} du dv$$

In general, $f(x,y)$ is a finite and positive 2-D sequence and $F(u,v)$ is a 2-D complex sequence. $F(u,v)$ can be represented in terms of a real part $\text{Re}\{F(u,v)\}$ and an imaginary part $\text{Im}\{F(u,v)\}$, or in terms of a magnitude part $M(u,v)$ and a phase part $\theta(u,v)$. $M(u,v)$ and $\theta(u,v)$ can be computed from,

$$M(u, v) = \sqrt{(\text{Re}(F(u, v)))^2 + (\text{Im}(F(u, v)))^2}$$

and

$$\theta(u, v) = \tan^{-1} \frac{\text{Im}(F(u, v))}{\text{Re}(F(u, v))}$$

Our study determines the different contributions of the magnitude and phase spectra to image synthesis and apply this knowledge to image processing.

Given a magnitude or phase spectrum, or both, it is of interest in image synthesis to find out the original image. The inverse Fourier transform provides a solution to the problem. Three kinds of synthesis may be classified: a complete synthesis, magnitude-only synthesis and phase-only synthesis. A complete synthesis may be derived when given both magnitude and phase spectra. It is,

$$f(x, y) = \mathcal{F}^{-1}\{M(u, v)e^{i\theta(u, v)}\}$$

where \mathcal{F}^{-1} is inverse Fourier transform. The magnitude-only synthesis is defined as

$$f(x, y) = \mathcal{F}^{-1}\{M(u, v)\}$$

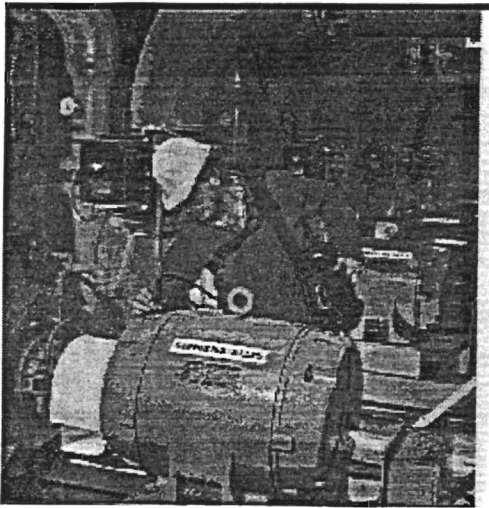
and phase-only synthesis is defined as

$$f(x, y) = \mathcal{F}^{-1}\{M_0(u, v)e^{i\theta(u, v)}\}$$

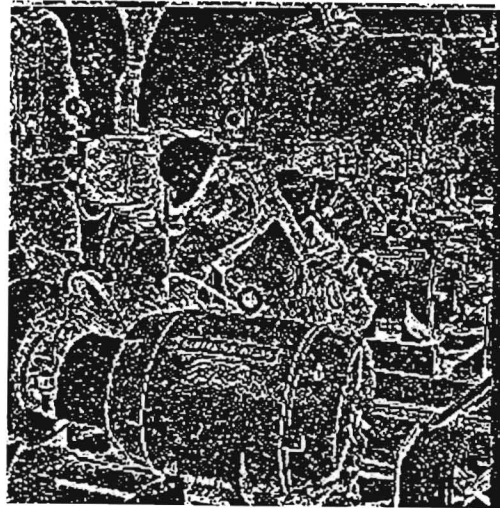
where $M_0(u, v)$ is the unity magnitude or the average of a class of similar images. It is based on the ergodic assumption of images which has been discussed in the ensemble average section of Chapter III.

(b) **Experiments.**—We begin with the synthesis of one single picture. First, we compute the Fourier transform of a single picture $f(x,y)$, then retrieve the magnitude $M(u,v)$ and phase $\theta(u,v)$ spectrum respectively, and finally, we carry out the magnitude-only and phase-only synthesis. For the phase-only synthesis, if the unit magnitude spectrum $M_0(u,v)$ is very small, say 1.0, the synthetic picture may be too dim to see and an appropriate factor for $M_0(u,v)$ will then be needed. The results are shown in Figure 4-1. This case tells us that the phase spectrum contains the most important feature of an image and the synthesis from the phase-only spectrum is very high in intelligibility (Figure 4-1b), while the magnitude spectrum is not (Figure 4-1c). This implies possible image reconstruction from phase-only information.

Let us look at the synthesis in crossing two different pictures. Following the same instructions above, we compute the magnitude and phase spectra of two pictures respectively, exchange the phase spectra of these two pictures and the magnitude spectra remain unchanged. The synthesized pictures are shown in Figure 4-2. This case highlights the previous statement again. The synthetic picture is determined by the corresponding phase spectrum and seems to have nothing to do with the magnitude spectrum. For example, the image (Figure 4-2c) synthesized from the phase spectrum of 'UWO' and the magnitude spectrum of 'MAN' (Figure 4-2a) looks close to its phase spectrum's picture 'UWO' (Figure 4-2b).



(a) The original picture 'MAN'



(b) The phase-only synthesis picture from the phase spectrum of 'MAN' and unit magnitude spectrum

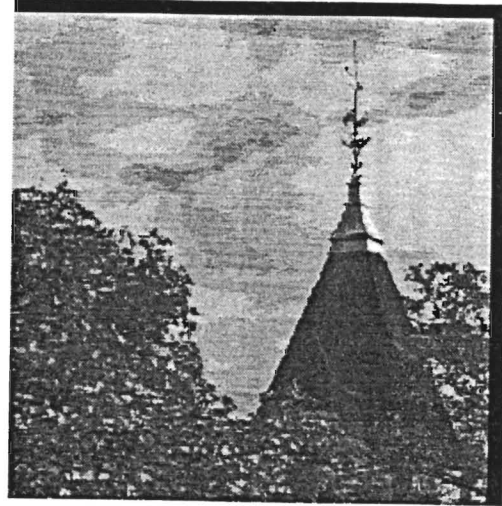


(c) The magnitude-only synthesis picture from the magnitude spectrum of 'MAN' and the zero phase

Fig. 4-1. Single picture's synthesis



(a) The original picture 'MAN'



(b) The original picture 'UWO'



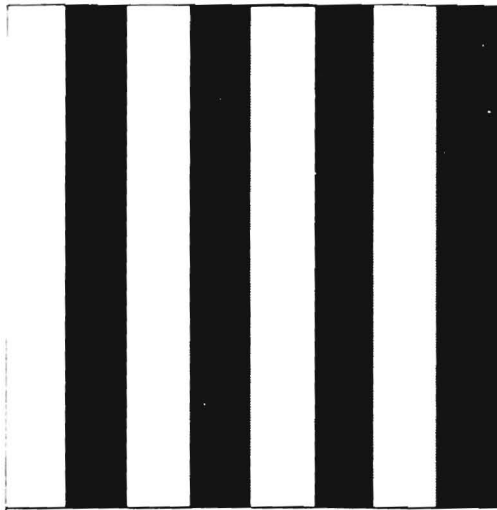
(c) The synthesized picture from the phase spectrum of 'UWO' and the magnitude spectrum of 'MAN'



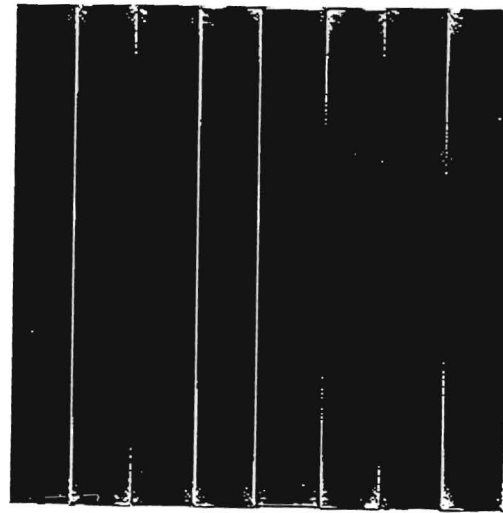
(d) The synthesized picture from the phase spectrum of 'MAN' and the magnitude spectrum of 'UWO'

Fig. 4-2. Pictures' cross synthesis

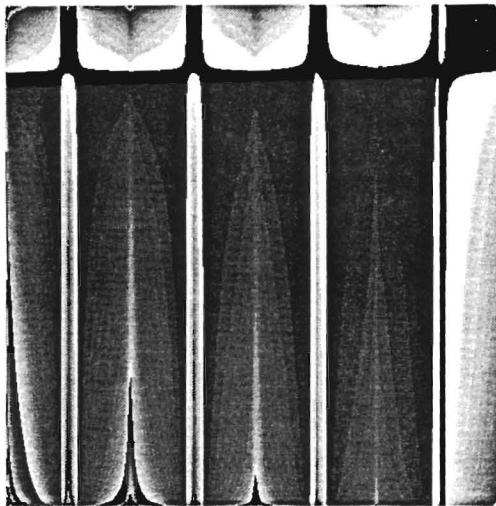
The two continuous grey tone pictures ('MAN' and 'UWO') above are very common in our daily lives. But still, there exist some special cases, like pictures with very high geometric structure and symmetric pictures. Let us choose two of these pictures and repeat the experiments above. The results are shown in Figure 4-3 and Figure 4-4 respectively. The weight of the test results seems to be put more on the magnitude side (Juvells, 1991). The magnitude-only synthesis has a good reconstruction (Figure 4-3c). What's more, the synthesized picture from the phase spectrum of 'BALL' (Figure 4-4c) doesn't look like the balls at all, but like some similar periodic bar information from its magnitude-contributed counterpart. Meanwhile the synthesis from the magnitude part of 'BALL' contains something that looks like the balls (Figure 4-4d). But still, there is another important characteristic of the phase spectrum. That is the phase information can give the correct location of the pixels in the spatial domain. The phase-only synthesis of a bar picture (Figure 4-3b) has a very sharp edge like its original picture (Figure 4-3a) and the synthesized picture from the phase spectrum of 'BALL' (Figure 4-4d) has three horizontal bars which implies the possible location of the balls in the horizontal direction. This is one significant feature of the phase spectrum. As we know, the shifting in spatial domain only effects the phase spectrum, it has nothing to do with the power spectrum. Another well-known case is when an IIR filter is applied to an image, the incorrect phase response may distort the edge information



(a) The original picture 'BAR'



(b) The phase-only synthesis picture from the phase spectrum of 'BAR' and unit magnitude spectrum

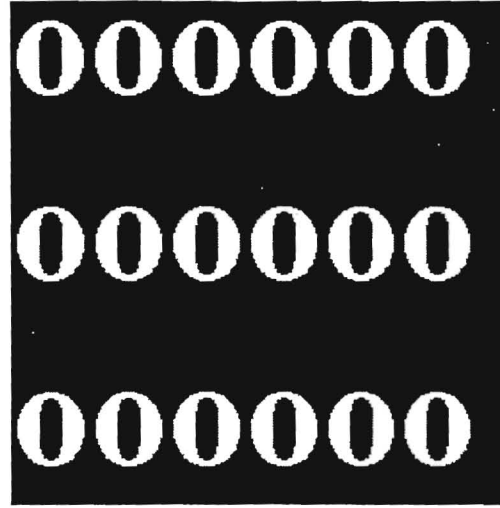


(c) The magnitude-only synthesis picture from the magnitude spectrum of 'BAR' and the zero phase

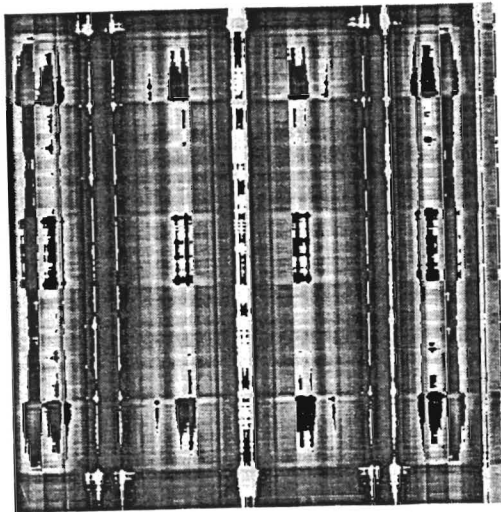
Fig. 4-3. Single high-geometry picture's synthesis



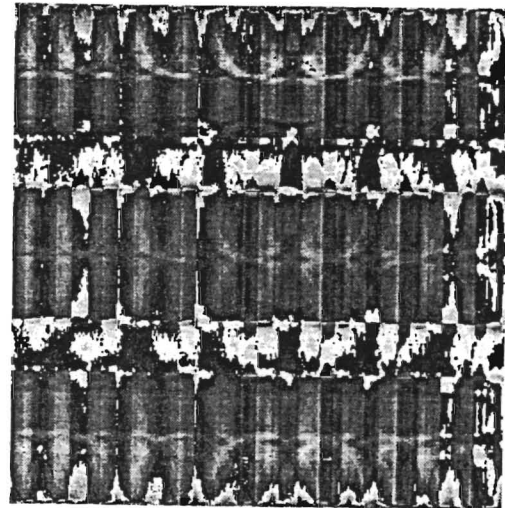
(a) The original picture 'BAR'



(b) The original picture 'BALL'



(c) The synthesized picture from the phase spectrum of 'BALL' and the magnitude spectrum of 'BAR'



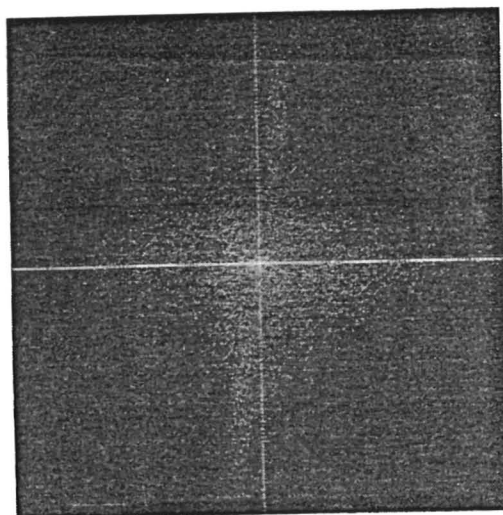
(d) The synthesized picture from the phase spectrum of 'BAR' and the magnitude spectrum of 'BALL'

Fig. 4-4. High-geometry picture's synthesis

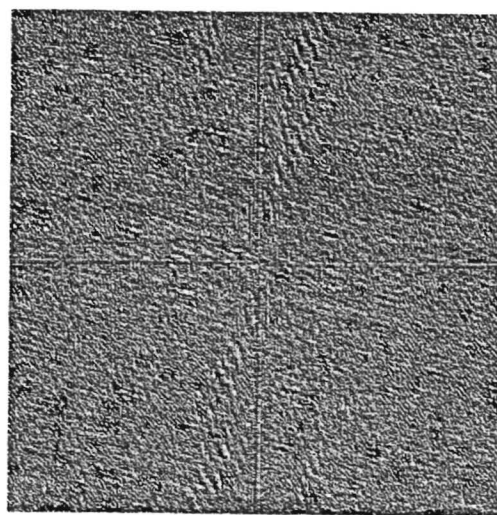
and result in a blurred profile image (Dudgeon et al., 1984).

In order to have a better understanding of these, it is helpful to look at the magnitude and phase spectra in the frequency domain. Figure 4-5 and Figure 4-6 illustrate the logarithms of the magnitude and phase spectra of 'UWO' and 'MAN', and 'BAR' and 'BALL' respectively. Surprisingly enough, all magnitude spectra are very high in intelligibility, while the phase spectra are not. But within a certain area near the zero frequency (the central part), the magnitude spectra of 'MAN' and 'UWO' are very similar (Figure 4-5a vs. Figure 4-5c). This is true for most continuous tone pictures. As for the phase spectra, they are different in texture and pixel' orientation. It is easier to see if we divide the spectra into blocks. Looking at the geometric pictures' spectra, the magnitude spectra reflect the significant geometric characteristics of the original pictures (Figure 4-6a vs. Figure 4-6c). The higher geometric structure in magnitude spectra allows them to play a more important role in image synthesis.

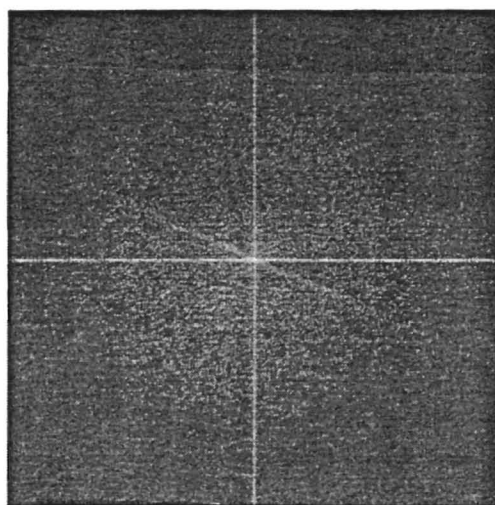
(c) Conclusion.—After a series of experiments, we have seen different roles played by the magnitude and phase spectra. Generally, the phase spectrum contains more important information of a picture and phase-only synthesis is higher in intelligibility. While for the geometric, periodic, or symmetric pictures, the magnitude spectrum contributes more to image synthesis.



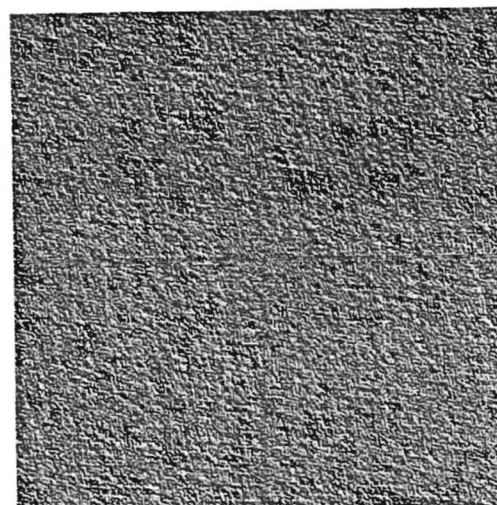
(a) The magnitude spectrum of 'MAN'



(b) The phase spectrum of 'MAN'

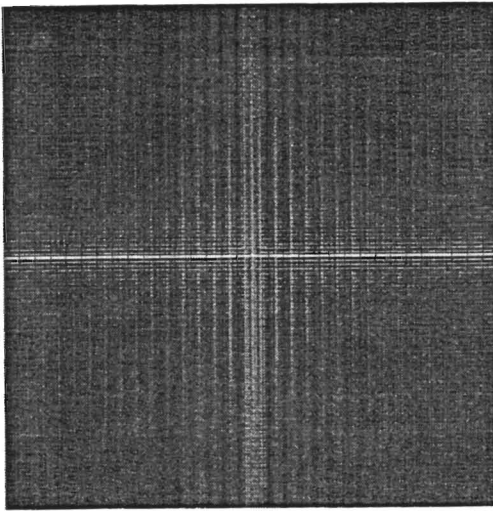


(c) The magnitude spectrum of 'UWO'

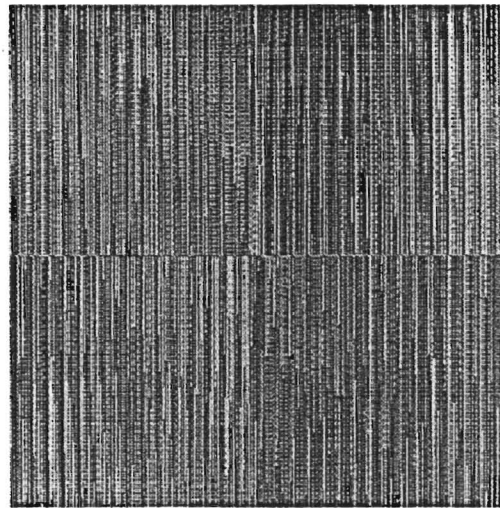


(d) The phase spectrum of 'UWO'

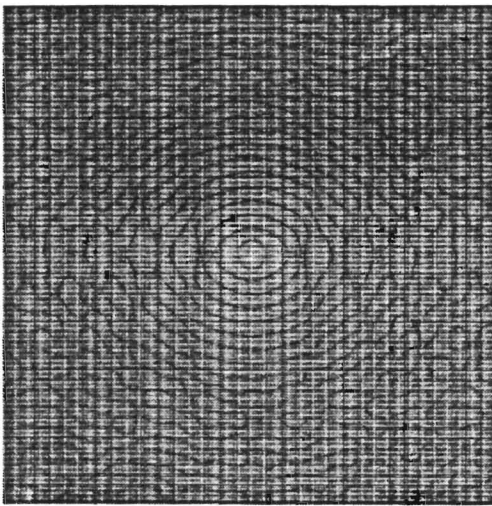
Fig. 4-5. Logarithm magnitude spectra of continuous grey tone pictures



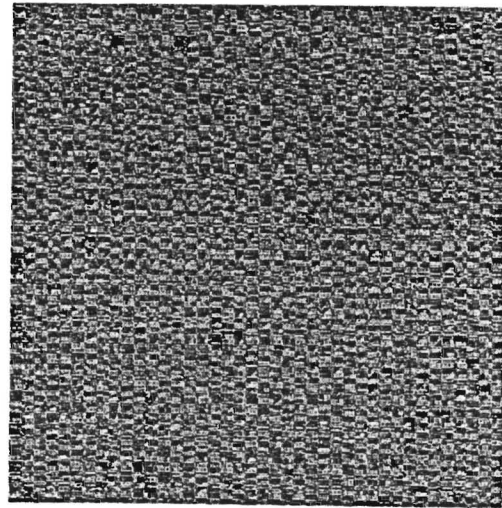
(a) The magnitude spectrum of 'BAR'



(b) The phase spectrum of 'BAR'



(c) The magnitude spectrum of 'BALL'



(d) The phase spectrum of 'BALL'

Fig. 4-6. Logarithm magnitude spectra of high-geometry pictures

Image restoration via a true phase spectrum

(a) **Introduction.**—As previously explained, the phase spectrum carries the most important information of an image and an image may be well reconstructed from its phase-only synthesis. One of the most successful applications is found in image restoration.

In Chapter III, a degraded picture is modeled as,

$$g(x,y) = h(x,y) ** f(x,y) + n(x,y)$$

If $h(x,y)$ is a zero phase or near zero phase operator, regardless of the sensitivity of the deviation from zero phase, the degraded picture has the same phase spectrum as that of the original one. Given this phase spectrum, the problem of restoration is to find the correct magnitude spectrum. One solution is based on power spectrum estimation. The other solution is based on the magnitude-only filter which will not change the correct phase spectrum.

Let us begin with the power spectrum estimation. Assume the absence of noise and $h(x,y)$ as a smoothing operator, since most degraded cases of computer simulation are generated by a lowpass or Gaussian filter. Then

$$g(x,y) = h(x,y) ** f(x,y)$$

Its Fourier transform is

$$G(u,v) = H(u,v) F(u,v)$$

Since the phase spectrum of $G(u,v)$ is the same as that of $F(u,v)$, only the true magnitude spectrum is left to be discovered in the restoration. Let the

degraded picture pass another zero phase smoothing filter, say $S(u,v)[\dots]$, then

$$S(u,v)[G(u,v)] = S(u,v)[H(u,v) F(u,v)]$$

Since $H(u,v)$ is also a smoothing operator, approximately

$$S(u,v)[G(u,v)] = H(u,v) S(u,v)[F(u,v)]$$

or

$$H(u, v) = \frac{S(u, v) [G(u, v)]}{S(u, v) [F(u, v)]}$$

then

$$F(u, v) = \frac{G(u, v)}{H(u, v)} = G(u, v) \frac{S(u, v) [F(u, v)]}{S(u, v) [G(u, v)]}$$

For most common pictures, the magnitude spectra look similar to each other (especially within a small area of the zero frequency). If we encapsulate a set of similar magnitude spectra's pictures into a class, then $S(u,v)[F(u,v)]$ can be regarded as a smoothing operator over the average spectrum of a set of pictures or over a very similar magnitude-spectrum-looking picture. It is obvious that the smoothing operator helps to reduce the dissimilarity among pictures of the same class, since the smoothed pictures only contain similar low frequency information. On the other hand, the smoothing operator $S(u,v)$ helps to prevent a large deviation from the original operator $H(u,v)$, it is easy to understand that the result of the convolution of two Gaussian filters is still

in the Gaussian shape, except different in width. So the approximation will be

$$F'(u, v) = G(u, v) \frac{S(u, v) |F_0(u, v)|}{S(u, v) |G(u, v)|}$$

where $|F_0(u, v)|$ and $|G(u, v)|$ are the magnitude spectra of the ensemble pictures or an arbitrarily similar magnitude spectrum picture and degraded picture respectively. The restored picture will be

$$f(x, y) = \mathcal{F}^{-1}(F'(u, v) e^{i\theta(u, v)})$$

Unlike the other methods introduced in the chapter on image restoration, this method does not require any a priori knowledge except a degraded picture $g(x, y)$ and a reasonable assumption of zero phase degradation. The principal challenge is power spectrum estimation. Compared to those algorithms, for example Wiener filter, this method seems to be poor. Rather, it is presented to reiterate the important feature of the phase spectrum and the similar power spectrum of most images.

Let us change to the restoration from magnitude-only filtering. Among all the restoration methods in Chapter III, both inverse filter (or so-called least square inverse filter) and Wiener filter (or so-called minimum mean square error (MMSE) filter) require one term of degraded filter $H(u, v)$, which may not be zero phase. Even though the original degraded filter $H(u, v)$ is a zero phase filter, the estimated of PSF (point spread function) estimation may be a non-

zero phase degraded filter. But all the experiments in image restoration of Chapter 3 are under the real degraded filters, which is the same as the assumption made in this section. The magnitude-only filters are of great interest, since they will not change the phase spectrum. Two of these types of filters are presented here: one is the so-called Wiener filter, which is a special case of MMSE filter when $H(u,v)$ is a delta function, that is $H(u,v)=1.0$, giving

$$M(u, v) = \frac{1.0}{1.0 + [|N(u, v)|^2 / |F(u, v)|^2]}$$

where $|N(u,v)|^2$ and $|F(u,v)|^2$ are power spectra of noise and original picture respectively. The Wiener filter is to remove degradation from additive noise. The other is a magnitude-only filter, which has the form

$$M(u, v) = \sqrt{\frac{|F(u, v)|^2}{|G(u, v)|^2}}$$

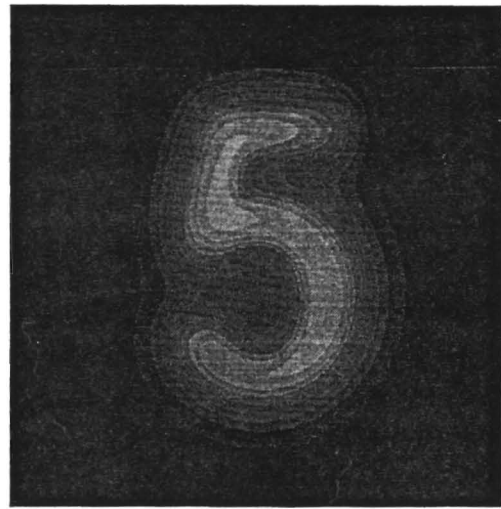
where $|G(u,v)|^2$ is the power spectrum of the degraded picture. The restored picture can be computed from

$$f(x,y) = \text{IDFT}[M(u,v) G(u,v)]$$

(b) Experiment.—The results of the power spectrum estimation are shown in Figure 4-7. The original filter $H(u,v)$ is a Butterworth low pass filter with a cutoff frequency at $6.0/512.0 \pi$, and the smoothing filter $S(u,v)$ is arbitrarily chosen to be the same type of filter with a cutoff frequency at $9.0/512.0 \pi$.



(a) The original picture '5'



(b) The picture degraded by a Butterworth lowpass filter

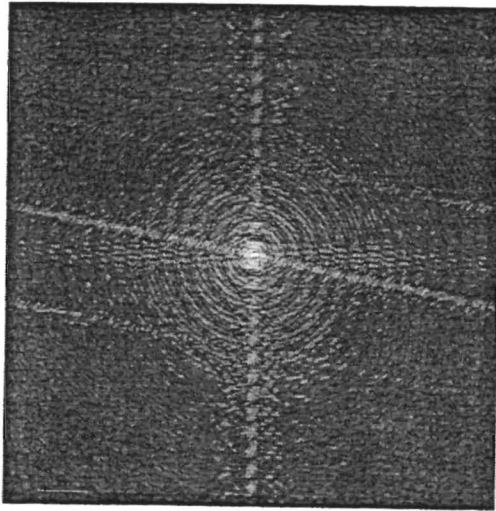


(c) An arbitrary picture '8' used for spectrum estimation

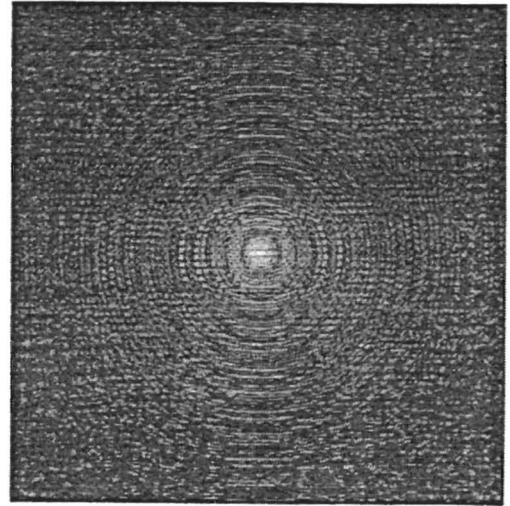


(d) The picture recovered by the power spectrum estimation

Fig. 4-7. Image restoration via power spectrum estimation



(e) The natural logarithm magnitude spectrum of '5'



(f) The natural logarithm magnitude spectrum of '8'

Fig. 4-7. (Continued)

Compared to the original picture (Figure 4-7a), the restored picture (Figure 4-7d) is well restored. The artifact of the restored picture is because of the contribution of picture '8' 's magnitude spectrum. While looking at the power spectra of '8' and '5', we find that in a small region of zero frequency, the power spectra of the original picture and the arbitrary picture are very similar (Figure 4-7d vs. 4-7f).

(c) Conclusion.—In a zero phase degraded situation, the phase spectrum of the degraded picture is the same as that of the original one. A restoration can be achieved with the correct phase spectrum and the estimated power spectrum. Among all the filters involved, only the magnitude-only filters and real zero phase filters are most appropriate in this case.

Image reconstruction from phase-only information

(a) Introduction.—The problem of this section is very similar to phase-only image synthesis and image restoration from its phase spectrum: an attempt to reconstruct a magnitude spectrum of an image close to original one. Since the phase spectrum is known, with an approximate magnitude spectrum, the image reconstruction is achieved. But the phase-only synthesis is made by means of a unit magnitude spectrum or the magnitude spectrum of ensemble images, while the phase-only image restoration is through the power spectrum

estimation over a degraded picture. Our task here is to find a direct relationship between magnitude and phase spectrum of an image. In some practical applications, for example, only the phase information is known. An example is a kinoform, a device to record the phase information of the scattered wavefront where the exact magnitude spectrum constructed from the phase spectrum is highly valuable and of great interest.

This question is similar to an interesting topic in DSP called spectral factorization, which is to recover a time or spatial domain sequence from its power spectrum or autocorrelation. Among all the sequences, only the minimum phase one is of interest, since the minimum phase sequence is a causal, stable and physically realizable system. A minimum phase sequence may be written as

$$S = \frac{(Z-Z_0)(Z-Z_1)\dots(Z-Z_n)}{(Z-P_0)(Z-P_1)\dots(Z-P_n)}$$

where all the zeros (Z_0, Z_1, \dots, Z_n) and poles (P_0, P_1, \dots, P_n) are outside the unit circle. Under the minimum phase constraint, the magnitude spectrum $M(\omega)$ and phase spectrum $\theta(\omega)$ are scale factors of Hilbert transforms of natural logarithms of each other,

$$\theta(\omega) = \Re[0.5 \ln (M(\omega))]$$

and

$$0.5 \ln (M(u,v)) = \Re[\theta(u,v)]$$

where \mathfrak{H} is the Hilbert transform. A detailed derivation and discussion can be found in Karl's book (1989)(Chapter 10 on spectral factorization).

The above statement is also true for a 2-D minimum phase sequence. But the discussion of a 2-D minimum phase sequence is not as straightforward as that in the 1-D case, due to the algebra's difficulty, that is the multidimensional polynomial cannot be generally factored. The power spectrum of the 1-D signal x is defined as

$$P(Z) = X(Z) X^*(Z^{-1})$$

where $*$ is the complex conjugate, and P and X are corresponding Z -transforms. If x is real, then

$$P(Z) = X(Z) X(Z^{-1})$$

To find out the 2-D sequence in this form is extremely difficult. However, there does exist such an expression in the 2-D case, called transcendental factorization (Dudgeon et al., 1984),

$$P(Z_1, Z_2) = X(Z_1, Z_2) X(Z_1^{-1}, Z_2^{-1})$$

But $X(Z_1, Z_2)$ has an infinite numbers of terms. In practice, the infinite terms of $X(Z_1, Z_2)$ will be a problem. For further study, let us change to a more convenient quantity, called the cepstrum $x'(n_1, n_2)$, which is defined as

$$x'(n_1, n_2) = \frac{1}{(2\pi i)^2} \int \int \ln X(Z_1, Z_2) Z_1^{n_1-1} Z_2^{n_2-1} dZ_1 dZ_2$$

The multiplication operation of the natural logarithm may be changed to the

addition operation, which helps to settle the problem in quadrants. Thus the transcendental factorization can be expressed as,

$$p'(n_1, n_2) = x'(n_1, n_2) + x'(-n_1, -n_2)$$

It is known that for multidimensional minimum phase sequences, their inverse and complex cepstra are absolutely summable and have the same region of support, which means the sequences are non-zero only in one quadrant of the (n_1, n_2) plane or a certain area, and will be zero outside that area (Dudgeon et al., 1984). The same region of support may be non-symmetric half-plane, etc. The same region of support is crucial to multidimensional minimum phase sequence. Since $p'(n_1, n_2) = x'(n_1, n_2) + x'(-n_1, -n_2)$ can be written as $x'(n_1, n_2) = p'(n_1, n_2) - x'(-n_1, -n_2)$. The condition for $x(n_1, n_2)$ to be both the minimum phase and finite term sequence is with the region of support in the first quadrant only, which is

$$x'(n_1, n_2) = \begin{cases} p'(n_1, n_2) & n_2 > 0 \text{ and } n_1 > 0 \\ 0.5 p'(n_1, n_2) & n_2 = 0 \text{ and } n_1 = 0 \\ 0 & \text{elsewhere} \end{cases}$$

This is the minimum phase constraint for 2-D sequences. However, many pictures of interest are not minimum phase sequence, which limits the application. But some other theorems (Quatieri, 1979) to broaden the class of such images, allow the exact magnitude reconstruction from the Fourier transform of its phase spectrum. These are listed below:

For 1-D case: For a sequence with no zero on the unit circle and no zero in conjugate reciprocal pairs, the magnitude spectrum is a scale factor of Fourier transform of its phase spectrum.

For 2-D case: For a finite $N_1 \times N_2$ points sequence with no symmetric factor in its Z-transform, the magnitude spectrum is a scale factor of $2N_1 \times 2N_2$ Fourier transform of its phase spectrum.

(b) Experiment.—The algorithm is very straightforward under the theorem mentioned above (Oppenheim, 1981). But the picture $f(x,y)$ must satisfy the following:

- (1) $f(0,0)$ is non-zero.
- (2) $f(x,y)$ will be zero outside the region of $0 \leq x \leq N_1-1$ and $0 \leq y \leq N_2-1$
- (3) No symmetric part in DFT and IDFT.

Then the algorithm is the following:

- (1) 2:1 zero padding the picture $f(x,y)$ to $f'(x,y)$
- (2) Compute and store the phase spectrum $\theta(u,v)$ of the picture $f'(x,y)$
- (3) Choose a unit magnitude spectrum $M_0(u,v)$
- (4) Compute $f'(x,y) = \mathcal{F}^{-1}(M(u,v)e^{i\theta(u,v)})$
- (5) Only take the first half of $f'(x,y)$ to store as $f(x,y)$
- (6) 2:1 zero padding $f(x,y)$ to $f'(x,y)$

- (7) Compute the magnitude spectrum $M(u,v)$ and new phase spectrum $\theta'(u,v)$ of the picture $f'(x,y)$, and discard the new $\theta'(u,v)$
- (8) Compute $f'(x,y) = \mathcal{F}^{-1}(M(u,v)e^{i\theta(u,v)})$
- (9) Only take the first half of $f'(x,y)$ to store as $f(x,y)$
- (10) Go back to (5) until a preselected number of iteration are completed.

The results are shown in Figure 4-8 and the reconstructed pictures (Figure 4-8c and Figure 4-8d) are much better than those done via the simple phase-only image synthesis and phase-only image restoration. After the sufficient iteration, there is almost no visual difference between the original picture (Figure 4-8a) and the reconstructed picture (Figure 4-8d).

(c) Conclusion.—Under the minimum phase condition, the magnitude can be exactly reconstructed from the Hilbert transform of its phase-only spectrum. And under some conditions as mentioned above, the magnitude can be exactly reconstructed by a scale factor of Fourier transform of its phase spectrum. The iterative method of eliminating the symmetric part of the image yields good results.



(a) The original picture 'MAN'



(b) The picture reconstructed from the phase spectrum of 'MAN' and the unit magnitude spectrum



(c) The picture reconstructed after 8 iterations



(d) The picture reconstructed after 50 iterations

Fig. 4-8. The iterative image reconstruction via the Fourier transform of the phase spectrum

Phase-only match filter and its applications

(a) **Introduction.**—Since the phase spectrum contains the most important information of an image and the image can be exactly constructed from its phase spectrum under a certain condition, can we apply this knowledge to a filter design? For example, first extract the phase spectrum from a signal, then design a filter based on its phase spectrum and use this filter to detect the desired signal. This is the problem of matched filter design.

The matched filter concept has many applications in DSP. It is particularly used in extracting the signal from the noise environment and improving the SNR. Here, the SNR is defined as the ratio between the power of the filter output when only signal is present and the power of the filter output when only noise is present,

$$SNR = \frac{\left| \int_{-\infty}^{\infty} s(t) ** h(t) dt \right|^2}{\left| \int_{-\infty}^{\infty} n(t) ** h(t) dt \right|^2}$$

where $s(t)$ is the signal, $n(t)$ is the noise and $h(t)$ is the filter respectively. SNR is a criterion for deriving the matched filter, and Karl's book (1989) gives the detailed derivation at pages 217-221. The general guideline is: first form the autocorrelation of noise Φ by multiplying the noise matrix $n(t)$ and its transpose $n^T(t)$, then in order to maximize the SNR performance, take the derivative with respect to filter's coefficient h_i , finally the result is given below,

$$\begin{pmatrix} \Phi_0 & \dots & \Phi_{n-1} \\ \vdots & & \vdots \\ \Phi_{n-1} & & \Phi_0 \end{pmatrix} \begin{pmatrix} h_0 \\ \vdots \\ h_{n-1} \end{pmatrix} = \begin{pmatrix} s_{n-1} \\ \vdots \\ s_0 \end{pmatrix}$$

So the crosscorrelation between the noise's autocorrelation and filter $h(t)$ is the reverse order of the signal sought to be detected. Thus $h(t)$ is called a correlator or a matched filter which searches for the desired signal in the noise. The autocorrelation of white noise is unity at zero lag and zero elsewhere. Thus,

$$h_i = s_{-i}$$

The Fourier transform of it will be

$$H(\omega) = S^*(\omega) = |S(\omega)| e^{-i\theta(\omega)}$$

Let $M(\omega)$ be the magnitude of $S(\omega)$, and obviously there exist three types of filters. The classical matched filter is

$$H(\omega) = M(\omega) e^{-i\theta(\omega)}$$

When $M(\omega) = 1.0$, the phase-only matched filter is

$$H(\omega) = e^{-i\theta(\omega)}$$

When $\theta(\omega) = 0$, the magnitude-only matched filter is

$$H(\omega) = M(\omega)$$

These matched filters can easily be expanded to 2-D case. Next, we discuss

the criteria for testing these filters:: Horner efficiency, peak height, noise immunity and discrimination ability.

Horner efficiency (Horner, 1984), also named optical efficiency, is defined as

$$\eta_H = \eta_m \frac{\int_{-\infty}^{\infty} \int_{-\infty}^{\infty} |f(x, y) ** h^*(x, y)|^2 dx dy}{\int_{-\infty}^{\infty} \int_{-\infty}^{\infty} |f(x, y)|^2 dx dy}$$

where η_m is the medium's efficiency and is taken as unity in this study. This criterion for the discrete case with a finite number of terms becomes

$$\eta_H = \frac{\sum_{x=0}^{n-1} \sum_{y=0}^{n-1} f(x, y) ** h^*(x, y)}{\sum_{x=0}^{n-1} \sum_{y=0}^{n-1} |f(x, y)|^2}$$

The autocorrelation and crosscorrelation can be very easily implemented by Fourier computing. Horner proved that the pure phase correlation filter has 100% light efficiency. Thus the phase-only matched filter has the full Horner efficiency; and the other two are considerably less.

The peak height is directly related to the power of the output. The matched filter forms the crosscorrelation with the incoming signal. If this filter is the reverse version of the signal, this correlation then becomes the autocorrelation of the signal whose Fourier transform is its power spectrum. Thus the

correlation part, the output energy is multiplied with the peak height. The classical matched filter has a unit or near unit height in the noise condition, while the peak of the phase-only matched filter is larger than that. This is why the phase-only correlator can increase the output energy compared to the classical correlator.

Among these three filters, the phase-only matched filter has the sharpest peak and the smallest sidelobes. The sharp peak assists in the precise location of a target, and the small sidelobes help to eliminate the judgement of the false targets which may be generated by the sidelobes.

The ability to discriminate close objects is subject to the peak character of matched filters and it can be defined as a different term Δ ,

$$\Delta = \frac{|\sum \Phi_{f,h} - \sum \Phi_{h,h}|}{\sum \Phi_{h,h}}$$

The greater the difference between the crosscorrelation $\Phi_{f,h}$ and the autocorrelation $\Phi_{f,f}$, the better the discrimination ability, thus a larger different Δ . The phase-only matched filter is much better than other matched filters in image identification.

Another image restoration method may be computed from the inverse Fourier transform of the product of a noise image and a matched filter in frequency domain. But the large peak of a matched filter might blur the edge and the sidelobes may wrongly contribute to the image. Only phase-only

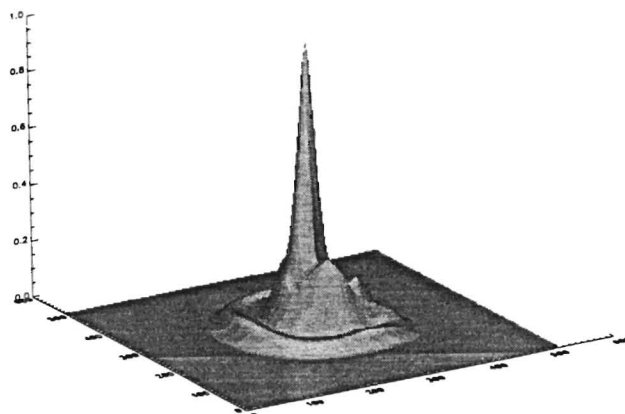
matched filter retains the best features of an image.

But the phase-only filter is not good for all cases. One of its big disadvantages is poor noise immunity. According to the phase shift theorem, a shift in the spatial domain will result in phase rotation in the frequency domain, leaving the power spectrum unchanged. So, the phase is very sensitive in the change of spatial positions. If a small amount of noise may be regarded as a change in position, the phase spectrum of the picture will be affected. This is why classical matched filters play an important role in low SNR situations. The experimental section will illustrate this effect.

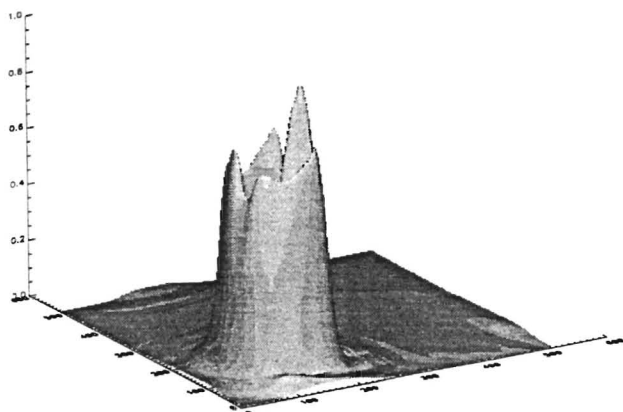
(b) Experiment.—The first part of the experiment is to observe the autocorrelation peaks of three matched filters. The crosscorrelation peak looks very close to that of the autocorrelation. The plots are viewed in Figure 4-9. We can see that the phase-only matched filter has the sharpest peak (Figure 4-9c) and classical matched filter (Figure 4-9b) is between the phase-only and the magnitude-only matched filters. And in $\text{SNR}=1.0$, the lower part of phase-only's autocorrelation is becoming noise-like (Figure 4-9f), but the peak is still sharp and contrasts sharply with the surroundings. When SNR gets worse, say $\text{SNR}=0.01$, the phase-only autocorrelation peak is completely buried in noise (Figure 4-9h), but classical and magnitude-only autocorrelation have some noise spots (Figure 4-9g and Figure 4-9i). Compared to the magnitude-



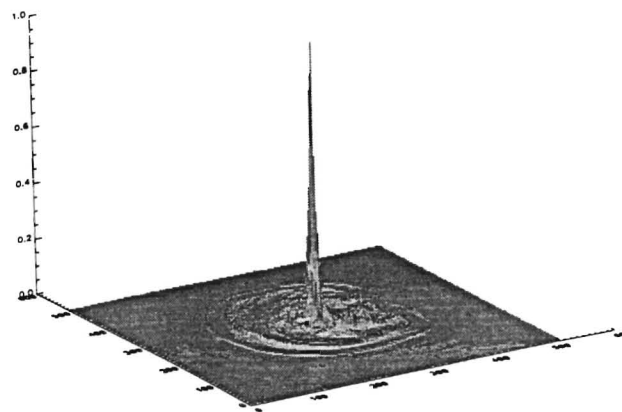
(a) The original picture 'G'



(b) Autocorrelation between the original picture and its classical matched filter

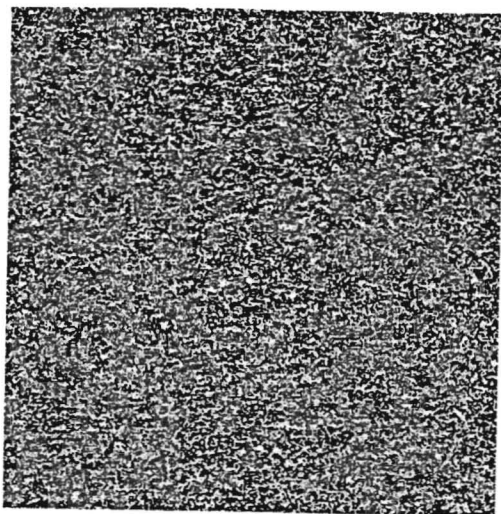


(c) Autocorrelation between the original picture and its magnitude-only matched filter

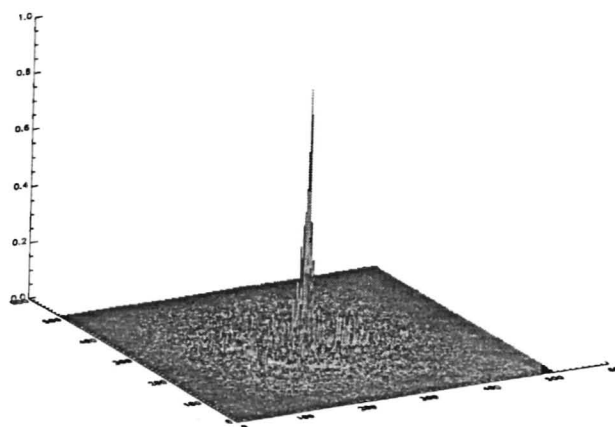


(d) Autocorrelation between the original picture and its phase-only matched filter

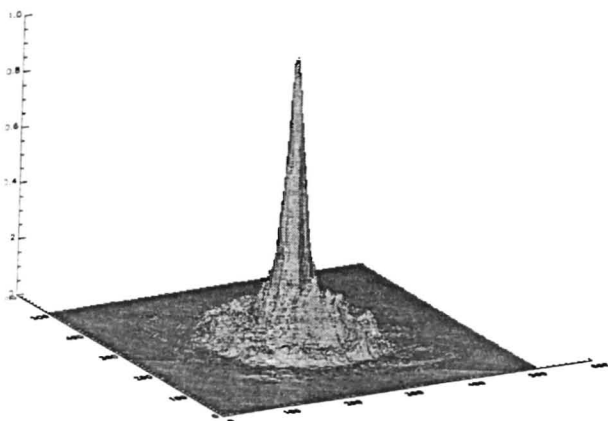
Fig. 4-9. Autocorrelation's peak of three match filters



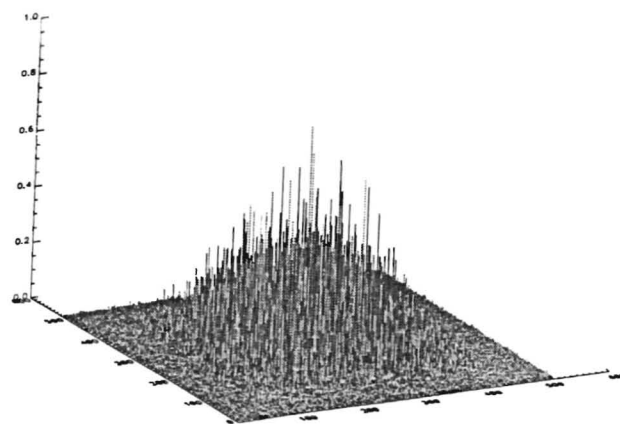
(e) The noise contaminated picture of 'G' with SNR = 1.0



(f) Autocorrelation between the noise picture and its phase-only matched filter with SNR = 1.0

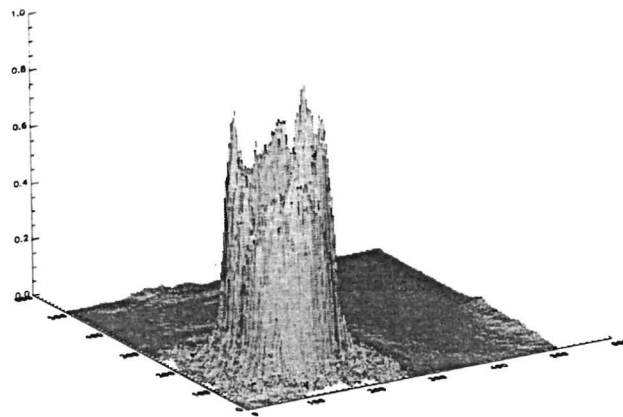


(g) Autocorrelation between the noise picture and its classical matched filter with SNR = 0.01



(h) Autocorrelation between the noise picture and its phase-only matched filter with SNR = 0.01

Fig. 4-9. (Continued)



- (i) Autocorrelation between the noise picture and its magnitude-only matched filter with $\text{SNR} = 0.01$

Fig. 4-9. (Continued)

only autocorrelation peak (Figure 4-9i), the classical one still has a quite clean peak (Figure 4-9g) in the central, especially the upper, part. This is why the classical matched filter can be applied in lower SNR environment, showing a modest detection because of its rather narrow peak. In order to remain consistent with the previous chapters, the SNR is still calculated from the ratio of the image variance to the noise variance.

The second part of the experiment is to test the matched filter's discrimination ability which is important in image identification and recognition. We will choose a set of pictures, ranging from very similar such as '3' versus '8', to completely dissimilar such as '3' versus '4', to the same character '3' versus the same character moved to the left, and to the noise situation such as '3' versus noise contaminated '3'. The pictures list in Figure 4-10 and the different terms Δ are calculated in Table 4-1.

Table 4-1 The discrimination test of three matched filters

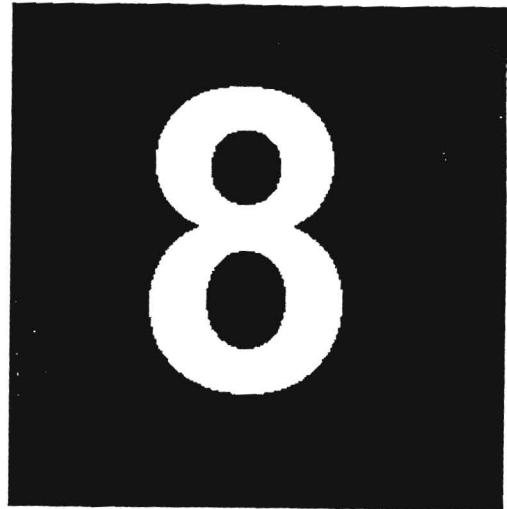
	3 vs. 8	3 vs. 4	3 vs. left 3	3 vs. noise 3
Classical	0.0961	0.8285	2.2053×10^{-7}	4.7591×10^{-4}
Phase-only	0.2608	6.1762	6.4120×10^{-5}	2.7460×10^{-3}
Magnitude-only	0.2244	0.0007	7.9502×10^{-6}	4.2060×10^{-4}

The test results show that only the phase-only matched filter can correctly distinguish the foreign objects from the desired object among all cases.

The last part of the experiment is image restoration via matched filters. It is



(a) Picture of '3'



(b) Picture of '8'



(c) Picture of '4'

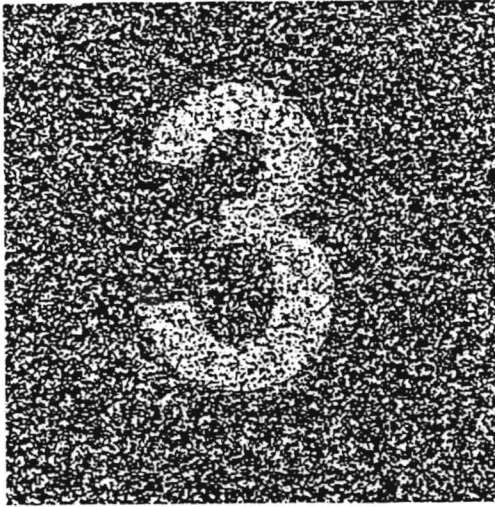


(d) Picture of '3' moved to the left

Fig. 4-10. Pictures for the discrimination ability test

shown in Figure 4-10. Compared to the restoration results shown before, these seem to be poor. Among the three filters, the phase-only matched filter does the best job (4-11c). Not only does it restore the location of the original picture, but also it contains the visible edge information of the original picture and has a rather high intelligibility. The classical matched filter also locates the correct position, but due to its large sidelobes and wider peak, the correct edge information cannot be easily retrieved (4-11b).

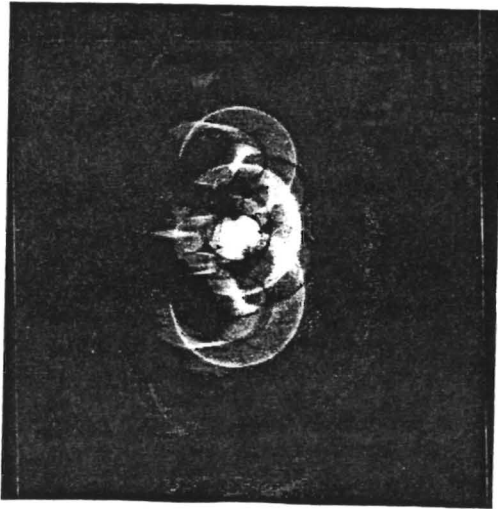
(c) Conclusion.—Under the criteria of Horner efficiency, peak height, noise immunity, and discrimination ability, the phase-only matched filter is superior to the others in a rather high SNR situation. This allows the phase-only matched filter to have valid applications in image recognition and image restoration. When the SNR decreases, the classical matched filter will be more advantageous than the phase-only filter.



(a) The noise contaminated picture of '3' with SNR = 1000



(b) The picture recovered from the classical matched filter



(c) The picture recovered from the phase-only matched filter



(d) The picture recovered from the magnitude-only matched filter

Fig. 4-11. Image restoration via matched filters

CHAPTER V

CONCLUSION

Digital image processing may be carried out in the spatial or frequency domain. In this study, filters in both domains were used. In particular, techniques in homomorphic image enhancement, image restoration and phase-only image processing were implemented and examples of each were presented.

Homomorphic filters are commonly employed for contrast enhancement, dynamic range compression, or both. The homomorphic filters of these three cases were applied to a picture 'TOWER' with the scattered background. The contrast enhancement improved the contrast of a background.

Inverse filters, Wiener filters and magnitude-only filters were applied to image restoration examples. When applied to the pictures degraded by a low-pass Butterworth filter and additive noise, the inverse filter restored the picture well in the high SNR case, but was not effective in the low SNR case. The inverse filter was also applied to small, medium and large frequency ranges for comparison. Good picture restoration was obtained when applied to the small neighborhood range, but restoration deteriorated as the neighborhood range was increased.

The Wiener filter is always superior to the inverse filter and its advantage increase as the SNR decrease. In addition, an improved method for deriving the Wiener filter in the spatial domain was developed.

Magnitude-only filters were applied to zero phase degradation. Ensemble averaging was used for the power spectrum estimation. Examples with different window size and overlap were presented. Optimal window size and overlap for improvement of frequency resolution and statistical resolution were obtained for the pictures tested.

Finally, magnitude-only and phase-only synthesis techniques were compared. High geometry pictures may be reconstructed from magnitude-only synthesis. For continuous tone pictures, phase-only synthesis was found to be preferred. A good image restoration may be found by the true phase spectrum and an estimated magnitude spectrum. The magnitude spectrum of an image may be exactly found by the Fourier transform of its phase spectrum. It was demonstrated that a phase-only matched filter is superior to other matched filters in Horner efficiency, peak height and discrimination ability. In the low SNR condition, the classical matched filter was shown to be more robust than phase-only matched filters.

REFERENCES

- Alexander, W.E., 1986, Spatial domain filters for image processing: Marcel-Dekker.
- Andrew, C.H., and Hunt, R.B., 1977, Digital image restoration: Prentice-Hall.
- Baxes, G.A., 1984, Digital image processing: Prentice-Hall.
- Cohen, M.F., and Wallace, J.R., 1993, Radiosity and realistic image synthesis: Academic Press.
- Dudgeon, D.E., 1984, Multidimensional digital signal processing: Prentice-Hall.
- Gonzalez, R.C., and Wintz, P., 1987, Digital image processing: Addison-Wesley.
- Hillery, A.D., and Chin, R.T., 1991, Iterative Wiener filters for image restoration: IEEE transaction on signal processing, Vol.39, No.5.
- Horner J.L., and Gianino, P.D., 1984, Phase-only matched filtering: Applied optics, Vol.23, 812-816.
- Juvells, L., Vallmitjana, s., Carnicer, A., and Campos, J., 1991, The role of amplitude and phase of Fourier transform in the digital image processing: Am.J.Phys., 59, 744-748.
- Karl, J.H., 1989, An introduction to digital signal processing: Academic press.
- Levune, M.D., 1985, Vision in man and machine: McGraw-Hill.
- Long, J., Yang, Z., Qiao, Z., 1992, Image processing under MS-Windows environment: B.S. thesis, Sun-yatsen University.
- Oppenheim, A.V., and Lim, J.S., 1981, The importance of phase in signals: Proceedings of the IEEE, Vol.69, 529-541.

Oppenheim, A., and Schafer, R.W., 1975, Digital signal processing: Prentice-Hall.

Quatietti, T. F., 1979, Phase estimation with application to speech analysis-Synthesis, Ph.D. dissertation, MIT.

Research system inc, 1993, IDL reference guide, Research system inc.

Research system inc, 1993, IDL user's guide, Research system inc.

Rosenfeld, A., 1982, Digital picture processing: Academic press.

Sezan, M.L., and Tekalp, A.M., 1990, Survey of recent development in digital image restoration: Optical engineering, 29, 393-404.

Stearns, S.D., and David, R.A., 1988, Signal processing algorithms: Prentice-Hall.

Watkins, C., 1993, Digital image processing : warping, morphing, and classical techniques: Academic Press.

APPENDIX

It is important to realize that Fourier transform matrix W discussed above is a transform matrix for matrix diagonalization and to understand some of its important properties.

Let's begin with a 3 elements circulant matrix H_C ,

$$H_C = \begin{bmatrix} h_1 & h_2 & h_3 \\ h_3 & h_1 & h_2 \\ h_2 & h_3 & h_1 \end{bmatrix}$$

and the eigenvalue of H_C is the DFT of its first row,

$$\lambda(k) = \text{DFT} \{h_1, h_2, h_3\} = \sum h(j) e^{-i2\pi kj/N},$$

notate W as $e^{-i2\pi kj/N}$, which will be a matrix as well,

$$W = \begin{bmatrix} 1 & 1 & 1 \\ 1 & W & W^2 \\ 1 & W^2 & W^4 \end{bmatrix}$$

and the inverse Fourier transform can be notated as the inverse matrix such as

$W^{-1} = (1/N) e^{i2\pi kj/N}$, then the result of $\lambda(k)$ would be,

$$\lambda(1) = h_1 + h_2 + h_3$$

$$\lambda(2) = h_1 + h_2 W + h_3 W^2$$

$$\lambda(3) = h_1 + h_2 W^2 + h_3 W^4$$

The diagonalization of matrix is of great interest, which is represented as

$$A H A^+ = \lambda$$

where A is the unitary transform, which means $A^+ = [A]^*{}^t = [A]^{-1}$, where * is the complex conjugate, ^t is the matrix's transpose, ⁻¹ is the inverse matrix and λ is the diagonal matrix. So multiply A on both sides,

$$A H A^+ A = A H = \lambda A$$

since

$$\lambda = \begin{bmatrix} \lambda(1) & 0 & 0 \\ 0 & \lambda(2) & 0 \\ 0 & 0 & \lambda(3) \end{bmatrix}$$

then

$$\lambda W = \begin{bmatrix} h_1+h_2+h_3 & h_1+h_2+h_3 & h_1+h_2+h_3 \\ h_1+h_2W+h_3W^2 & W(h_1+h_2W+h_3W^2) & W^2(h_1+h_2W+h_3W^2) \\ h_1+h_2W^2+h_3W^4 & W^2(h_1+h_2W^2+h_3W^4) & W^4(h_1+h_2W^2+h_3W^4) \end{bmatrix}$$

and

$$A W = \begin{bmatrix} h_1+h_2+h_3 & h_1+h_2W+h_3W^2 & h_1+h_2W^2+h_3W^4 \\ h_3+h_1+h_2 & h_3+h_1W+h_2W^2 & h_3+h_1W^2+h_2W^4 \\ h_2+h_3+h_1 & h_2+h_3W+h_1W^2 & h_2+h_3W^2+h_1W^4 \end{bmatrix}$$

Please note W is wrapped around and modulated by N=3, for example, $W^8 = W^{6+2} = W^2$, and $W^4 = W^{3+1} = W$. It is obvious to see that the results of $\{\lambda W\}$ and $\{W H\}$ are transposes with each other. Let's go back to the above expression.

$$A H A^+ = \lambda$$

taking the transpose on both sides. Since λ is the diagonal matrix and its transpose remains unchanged, A and A^+ are symmetric matrices, so their transposes remain unchanged. Thus

$$A H^t A^+ = \lambda$$

With the above expression, it turns out that the diagonalization matrix A is the Fourier transform matrix W . This important conclusion may help to find a fast matrix operation to be implemented by DFT or faster FFT based on their eigenvalues.

Since $W H W^+ = \lambda$ may be written as $W H = \lambda W$, according to the definition that if $A X = \lambda X$, then X is the eigenvector of matrix A . So W is the eigenvector of matrix H .

There is one important property from the above result,

$$W H W^{-1} = \lambda \text{ or } H = W^{-1} \lambda W$$

taking the transpose on both sides,

$$H^t = W^{-1} \lambda W$$

then taking the complex conjugate on both sides again,

$$H^{t*} = [W^{-1}]^* \lambda [W]^*$$

since H is a real matrix, so $H^{t*} = H^t$ and

$$[W^{-1}]^* = (1/N) [W] \text{ and } [W]^* = N [W^{-1}]$$

So,

$$H^t = W \lambda^* W^{-1}.$$

The transpose of a circulant matrix is the transform of the complex conjugate of its diagonal matrix λ . We also can directly verify that $H^t = H^*$.

The circulant matrix can be viewed as a set of delay operators $\{D \dots\}$, such as $D^0 = h_1$, $D^1 = h_2$, and $D^2 = h_3$. Then

$$H_C = \begin{bmatrix} D^0 & D^1 & D^2 \\ D^2 & D^0 & D^1 \\ D^1 & D^2 & D^0 \end{bmatrix}$$

and its complex conjugate would be,

$$H_C^* = \begin{bmatrix} D^0 & D^{-1} & D^{-2} \\ D^{-2} & D^0 & D^{-1} \\ D^{-1} & D^{-2} & D^0 \end{bmatrix}$$

Since H_C^* is circulant, the wraparound will result in: $D^0 = h_1$, $D^{-1} = h_3$ and $D^{-2} = h_2$.

$$H_C^* = \begin{bmatrix} h_1 & h_3 & h_2 \\ h_2 & h_1 & h_3 \\ h_3 & h_2 & h_1 \end{bmatrix}$$

Obviously, it is the transpose of the original matrix, so

$$H^* = H^t$$